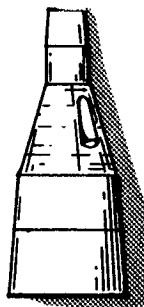


Copy No. 42

NASA Program Gemini Working Paper No. 5012

ANALOG SIMULATION OF GEMINI-PARAGLIDER EARTH
LANDING SYSTEM AND GROUND CONTROL FACILITY



FOR NASA
PERSONNEL ONLY

N75-70508

(NASA-TM-X-72209) ANALOG SIMULATION OF
GEMINI-PARAGLIDER EARTH LANDING SYSTEM AND
GROUND CONTROL FACILITY (NASA) 86 P

00/98 Unclas
17460

DISTRIBUTION AND REFERENCING

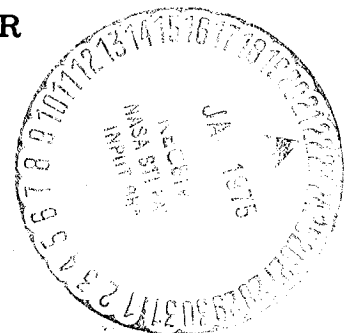
This paper is not suitable for general distribution or referencing.
It may be referenced only in other working correspondence and
documents by participating organizations.



NATIONAL AERONAUTICS AND SPACE ADMINISTRATION
MANNED SPACECRAFT CENTER

Houston, Texas

May 22, 1964



NASA PROGRAM GEMINI WORKING PAPER NO. 5012

ANALOG SIMULATION OF GEMINI-PARAGLIDER EARTH
LANDING SYSTEM AND GROUND CONTROL FACILITY

Prepared by: Herbert G. Patterson
Herbert G. Patterson
AST, Systems Analysis Branch

Authorized for Distribution:

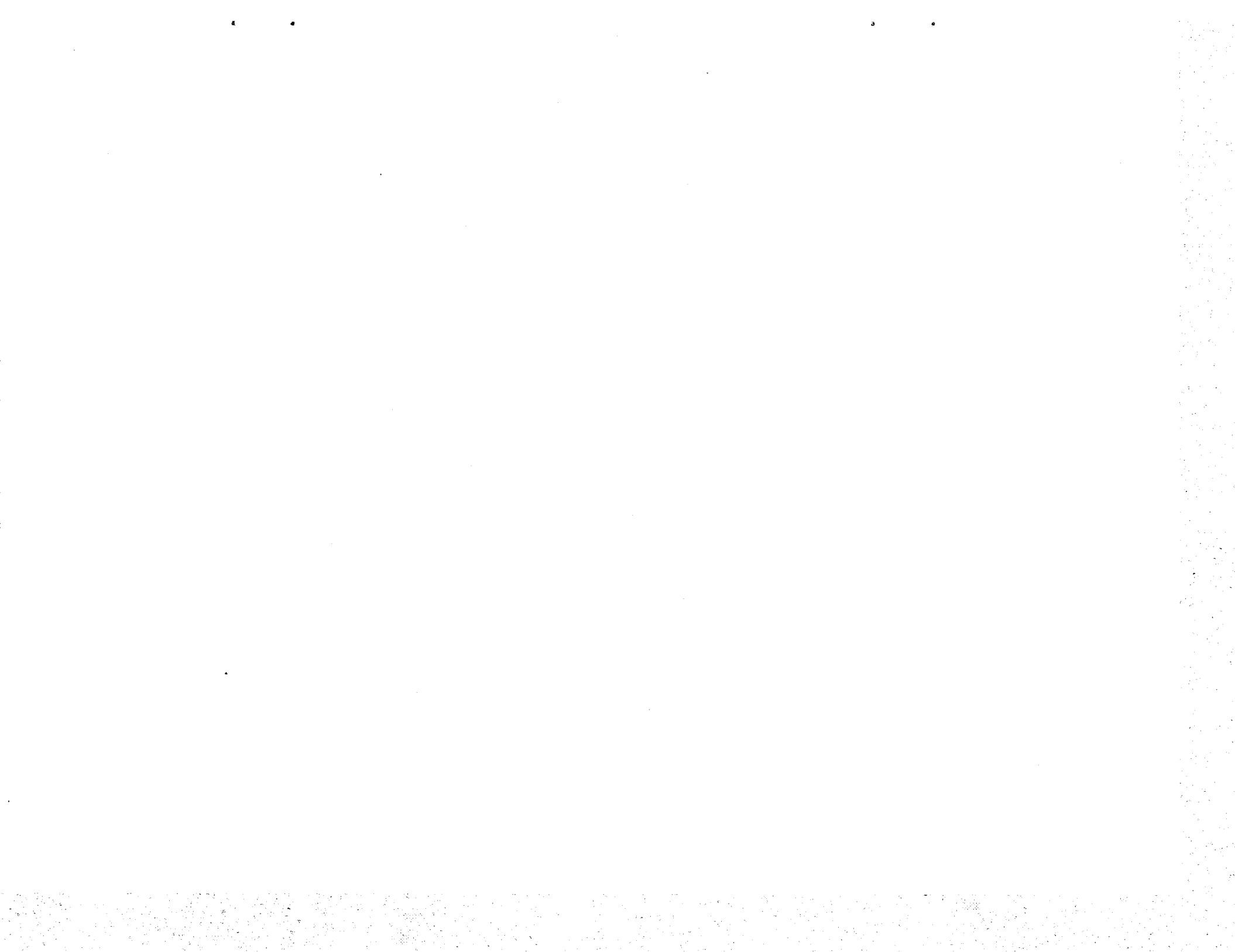
Warren Gillespie, Jr.
for Maxime A. Paget
Assistant Director for Engineering and Development

NATIONAL AERONAUTICS AND SPACE ADMINISTRATION

MANNED SPACECRAFT CENTER

HOUSTON, TEXAS

May 22, 1964



ABSTRACT

Describes an analog simulation of Gemini-paraglider earth landing system and ground control facility. Results of this study indicated a simple guidance scheme based on measured wind profiles and spacecraft performance was sufficient for a landing controller to direct the vehicle to a landing site within its area of capability.

TABLE OF CONTENTS

Section	Page
SUMMARY	1
INTRODUCTION	1
LIST OF SYMBOLS	2
VEHICLE SIMULATION	6
Characteristics of Simulated Vehicle	6
Equations of Motion	6
Control System	6
Simulator Cockpit	8
TERMINAL LANDING SYSTEM SIMULATION	9
Guidance Routine	9
Displays	11
TEST PROCEDURES	13
General	13
Recorded Data	13
DETERMINATION OF VEHICLE PERFORMANCE AND NORMAL OPERATING PROCEDURES	16
Vehicle Performance	16
Normal Operating Procedures	17
RESULTS AND DISCUSSION	18
Radar Accuracies	18
Wind Effects	19
Initial Position	21
Cross Wind	22
System Failures and Alternate Procedures	23
Automatic Direction Finding (ADF)	29
Display Areas	30
Computer Functions	32
CONCLUDING REMARKS	32

Section	Page
REFERENCES	36
APPENDIX A EQUATIONS OF MOTION	37
Force Equations	37
Moment Equations	38
Aerodynamic Forces	38
Vehicle Attitude Angles	38
Vehicle Attitude Angles	38
Velocities With Respect to Air Mass	38
Vehicle Position	39
Additional Equations	39
Constants	39
Vehicle Inputs	39
Functions of h	40
Functions of α_k	40
Control Inputs	40
APPENDIX B AERODYNAMIC DATA	41

LIST OF TABLES

Table		Page
I	Physical Characteristics of Gemini Spacecraft Simulated	42
II	Test Cases	43

LIST OF FIGURES

Figure		Page
1	Block diagram of analog simulation	45
	a. Computer math flow	45
	b. Pilot-controller information flow	46
2	General dimensions of simulated vehicle	47
3	Body and earth fixed axes systems	48
4	Change in lateral shroud length (l_r) versus stick deflection in roll (δ)	49
5	Change in trim angle of attack (α_t) versus stick deflection in pitch (ϵ)	50
6	Lift to drag ratio (L/D) versus keel angle of attack (α_K)	51
7	Capsule angle of attack (α_c) versus keel angle of attack (α_K)	52
8	Simulator cockpit	53
9	Hand controller.	54
	a. Resultant motion	54
	b. Pilot's hand position	55
10	Display panel	56
	a. Complete console	56
	b. Command astronaut's console	57
11	Wind profiles used in the simulation	58
	a. Summer winds	58
	b. Winter winds	59
12	Maximum available range versus altitude	60

Figure	Page
13	Terminal landing system simulation 61
14	Preselected target plus surrounding area (30 in. by 30 in. X-Y plotter) 62
15	Ellington Air Force Base (10 in. by 15 in. X-Y plotter) 63
16	Preselected runway (10 in. by 15 in. X-Y plotter). . . . 64
17	Final approach altitude versus range (10 in. by 15 in. X-Y plotter). 65
18	Ling-Temco-Vought display system 66
	a. Complete console 66
	b. 15 in. by 15 in. display screen. 67
19	Radar altitude and predicted heading instruments 68
20	Altitude versus rate of descent. 69
21	Altitude versus air speed. 70
22	Altitude versus turn rate. 71
23	Altitude versus turn radius. 72
24	Ground trace of vehicle (Run A-2). 73
25	Altitude versus range trace of vehicle (Run A-2) 74
26	Time histories of terminal descent (Run A-2) 75
	a. Eight channel recorder (A) 75
	b. Eight channel recorder (B) 76
27	Miss distance during final approach. 77
28	Aerodynamic force coefficients (C_X , C_Z) versus keel angle of attack (α_K). 78

ANALOG SIMULATION OF GEMINI-PARAGLIDER EARTH
LANDING SYSTEM AND GROUND CONTROL FACILITY

SUMMARY

The terminal descent and landing approach control of the Gemini-paraglider earth landing system was studied utilizing facilities assigned to the Guidance and Control Division. A fixed-base simulator containing a hand-controller and pilot displays was used to represent the Gemini-paraglider earth landing system. Analog X-Y plotting equipment was used to depict the ground control facility or terminal landing system. In addition, the application of a commercially available projection display system in the terminal landing system was evaluated. The six degrees-of-freedom equations of motion were solved utilizing an analog computer.

Results of this study indicated that a simple guidance routine, based on integration of measured wind profiles and the lift-to-drag ratio of the spacecraft, was sufficient to predict the vehicle's center of capability and area of capability. Based on this information, the terminal landing system operator could direct the spacecraft to a preselected landing site within the area of capability. Except for the condition where severe wind gusts at the landing site caused the spacecraft to become uncontrollable, the operator could also direct the spacecraft during final approach so that the flight terminated on the desired runway.

INTRODUCTION

The function of the Gemini-paraglider earth landing system is to give the spacecraft the ability to land at a preselected landing site after reentry through the earth's atmosphere. The ability of the spacecraft to achieve such a landing depends not only upon the accuracy of the navigation system prior to an atmospheric reentry and the accumulation of errors during reentry, but also upon the performance of the spacecraft after emergence from blackout. Because of the flight characteristics of the Gemini-paraglider and the possibility of unfavorable weather condition at the landing site, there is a necessity for a terminal landing system to enhance the possibility of performing a successful descent and landing during the terminal phase of the mission. It is conceived that the terminal landing system would consist of several mobile units that would be stationed at the primary landing site sometime prior to spacecraft reentry. The units will be

self-contained including their own wind measuring and radar devices. Upon emergence from blackout, the terminal landing system operator will communicate with the pilot and guide the spacecraft to the landing site. The controlled terminal descent may be further complicated by considerations of wind effects, accuracies of wind measuring device, accuracies of radar equipment, initial spacecraft position at paraglider deployment, system failures, et cetera.

A study of the feasibility of a ground controlled approach of the Gemini-paraglider earth landing system was undertaken by the Systems Analysis Branch of the Guidance and Control Division. This study consisted of an analog simulation of both the terminal landing system and Gemini-paraglider earth landing system. The objectives of the study were to:

1. Determine a terminal guidance technique and operational procedures for support of the terminal phase of the Gemini-paraglider earth landing system.
2. Develop functional specifications for the subsystems required to implement the guidance routine and operational procedures.
3. Determine the display equipment required onboard the terminal landing system.
4. Determine the application of wind profile information to the guidance technique that would be used during the terminal descent and a method of computing the bias target corrections that would be applied prior to atmospheric reentry.

The author wishes to acknowledge the assistance of Mr. Darwin E. Crawford of the Computer Simulation Section, Simulation Branch, Guidance and Control Division who programed and mechanized the equations used in this study; also, Messrs. John G. Zarcaro, Jerry L. Lowery, and Jackson B. Craven of the Landing Operations and Facilities Section, Recovery Branch, Landing and Recovery Division who provided valuable technical support during the study.

LIST OF SYMBOLS

A_t	Azimuth angle between the center of capability and the target, deg
C_1, C_2, C_3	Arbitrary constants

$C_{l\beta}$	Rate of change of rolling moment coefficient with sideslip angle
C_{lp}	Rate of change of rolling moment coefficient with rolling velocity
$C_{l\Delta}$	Rate of change of rolling moment coefficient with change of lateral shroud length
C_{mq}	Rate of change of pitching moment coefficient with pitching rate.
$C_{m\alpha}$	Rate of change of pitching moment coefficient with angle of attack
$C_{n\beta}$	Rate of change of yawing moment coefficient with sideslip angle
C_{nr}	Rate of change of yawing moment coefficient with yawing rate.
$C_{n\Delta}$	Rate of change of yawing moment coefficient with change of lateral shroud length
C_x	Force coefficient along X_b
$C_{y\beta}$	Rate of change of force coefficient along Y_b with angle of sideslip
$C_{y\Delta}$	Rate of change of force coefficient along Y_b with change in lateral shroud length
C_z	Force coefficient along Z_b
d	Vehicle reference length, ft
f	Fuel, lb
g	Gravitational acceleration, ft/sec ²
h	Altitude ($-Z_e$), ft
I_x, I_y, I_z	Moments of inertia about X_b, Y_b, Z_b , slug-ft ²

I_{xz}	Product of inertia in the $X_b - Z_b$ plane, slug-ft ²
L/D	Lift to drag ratio
l_1, l_2, l_3	Longitudinal shroud lines, ft
l_k	Keel length, ft
l_r	Lateral shroud line, ft
m	Mass of vehicle, slugs
p, q, r	Vehicle angular velocities about X_b, Y_b, Z_b , rad/sec
\bar{q}	Dynamic pressure, lb/ft ²
R	Radius of the maximum available range, ft
S	Vehicle reference area, ft ²
u, v, w	Vehicle velocities along X_b, Y_b, Z_b , ft/sec
$\bar{u}, \bar{v}, \bar{w}$	Vehicle velocities with respect to air mass, ft/sec
V_i	Indicated air speed, ft/sec
V_t	Total velocity, ft/sec
W_x, W_y	Vehicle wind profiles in the X_e and Y_e directions, ft/sec
W_{x_p}, W_{y_p}	Measured wind profiles in the X_e and Y_e directions, ft/sec
X_a, Y_a, Z_a	Aerodynamic forces along X_b, Y_b, Z_b , lb
X_b, Y_b, Z_b	Vehicle body axes
X_e, Y_e, Z_e	Vehicle position in the earth fixed axes, ft

X_p, Y_p	Center of capability in the X_e and Y_e directions, ft
X_r, Y_r, Z_r	Radar position along X_e, Y_e, Z_e , ft
X_T, Y_T	Target position along X_e, Y_e , ft
\bar{X}	Longitudinal center of gravity position, in.
\bar{Y}	Lateral center of gravity position, in.
α_c	Capsule angle of attack, deg
α_k	Keel angle of attack, deg
α_t	Trim angle of attack, deg
$\alpha_{t \text{ D.B.}}$	Deadband about command α_t , deg
β	Sideslip angle, deg
Γ	Range of vehicle to target, ft
γ	Flight path angle, deg
Δ	Change in lateral shroud lines, in./in.
Δh	Altitude lost for a 180 degree turn, ft
$\Delta_{\text{D.B.}}$	Deadband about commanded Δ , in./in.
δ	Stick deflection in roll, deg
ϵ	Stick deflection in pitch, deg
ρ	Atmospheric density, slugs/ft ³
σ	Density ratio, ρ/ρ_0
Ψ, θ, ϕ	Vehicle attitude angles, deg

A dot over a variable denotes first derivative with respect to time.

VEHICLE SIMULATION

The terminal descent of the Gemini-paraglider earth landing system was implemented by coupling an analog computer solution of the spacecraft equations of motion to a fixed-base partial simulation of the Gemini cockpit. The cockpit included pilot displays, a three-axes hand controller, and a command astronaut's chair. A block diagram of the analog simulation is shown in figure 1. A detailed description of the Gemini-paraglider may be found in reference 1.

Characteristics of Simulated Vehicle

The vehicle considered was a Gemini-paraglider earth landing system and had the physical characteristics presented in table I.

The general dimensions of the simulated vehicle are shown in figure 2.

Equations of Motion

The equations of motion (Appendix A) were written in six degrees-of-freedom and assumed a flat earth model. A diagram of the vehicle axes system and the earth fixed axes system is presented in figure 3. Wind velocities (W_x , W_y) and atmospheric density were programed as functions of altitude, and the aerodynamic force coefficients (C_x , C_z) were programed as functions of paraglider angle of attack (α_k). The aerodynamic coefficients used in the simulation were obtained from references 2 through 5 and from informal discussions with personnel of North American Aviation and are presented in Appendix B.

Control System

Following paraglider deployment, attitude control is accomplished by lengthening or shortening the shroudlines connecting the paraglider and Gemini spacecraft. These shroudlines are controlled by gas operated winches manually activated by the pilot through the Gemini hand controller. The paraglider control system has pitch and roll capabilities, but no yaw control.

Roll Control.- Roll control maneuvers were performed by changing the length of the diagonal or lateral shroud lines l_r . The change in length of the lines rolls the paraglider with respect to the Gemini spacecraft and in turn produced a banking maneuver. The rate of change of the line length was 9 in./sec and was assumed to be constant

while the winch is in operation. The time required for the winch to attain this 9 in./sec is small and was neglected in the study. Stick deflections to the right produce a shortening of the right lateral shroud line and in turn produce banking maneuvers to the right. The maximum deflection of the stick in roll was $\pm 10^\circ$ which shortens or lengthens the lateral shroud line by $(\pm \Delta = \pm l_r / l_k = \pm .04 \text{ in./in.})$.

Changes in lateral shroud line length, as indicated in figure 4, are directly proportional to stick deflection (ϵ). There is a deadband of 1 inch about the commanded shroud line length which corresponds to ($\Delta_{\text{D.B.}} = \pm .0027 \text{ in./in.}$). The hand controller has a deadband about the neutral position (upright position) of $\pm .5^\circ$. Therefore, if the stick is deflected in roll greater than $\pm .5^\circ$, the lateral shroud lines length changes at a rate of 9 in./sec ($\dot{\Delta} = .02452 \text{ (in./in.)}/\text{sec}$) until the actual length reaches the command length (plus or minus the 1 in. deadband).

Pitch Control. - Pitch control maneuvers were performed by changing the length of the longitudinal shroud lines l_1 and l_3 . These shroud lines are connected to the same control winch and therefore if l_1 is lengthened by a given amount, l_3 is shortened by the same amount. The longitudinal shroud lines were either lengthened or shortened by movement of the hand controller fore and aft of the neutral position (upright position). This in turn changed the trim angle of attack (α_t) and lift/drag ratio of the vehicle (L/D). The maximum deflection of the stick in pitch was $\pm 10^\circ$, which changed the longitudinal shroud line length by $(\pm \Delta l_1 / l_k = \pm .04 \text{ in./in.})$. Changes in longitudinal shroud line length and trim angle of attack (α_t) were directly proportional to stick deflections in pitch (ϵ) as shown in figure 5. Changes in L/D due to changes in keel angle of attack (α_k) are presented in figure 6 and changes in spacecraft angle of attack (α_c) with keel angle of attack are presented in figure 7. The reason for the difference between the change in keel angle of attack and change in spacecraft angle of attack for a given stick deflection in pitch is due to the geometric change in the configuration caused by longitudinal rigging of the support and shroud lines. There was a deadband of 1 inch about the commanded shroud line length which corresponded to a trim angle of attack deadband of ($\alpha_{\text{t D.B.}} = \pm .8 \text{ deg}$). Therefore, if the stick was deflected in pitch greater than $\pm .5^\circ$ (pitch deadband), the longitudinal shroud lines would lengthen or shorten at a rate of 9 in./sec which changed the trim angle of attack at a rate of ($\dot{\alpha}_t = 7.6 \text{ deg/sec}$) until the shroudline length reached the commanded length plus or minus the 1 inch deadband.

Simulator Cockpit

The simulator cockpit used in the simulation consisted of the command astronaut's seat, hand controller, and spacecraft display panel. The cockpit was surrounded by a curtain and the only communication to the pilots was through the intercommunication system between the simulator room and the analog computer room. The simulator cockpit is shown in figure 8. A complete description of actual cockpit can be obtained from reference 6.

Command Astronaut's Chair.- The command astronaut's chair used in the simulation was a transport aircraft pilot seat modified to erect the pilots in the proper position with respect to the display panel and control handle.

Hand Controller.- The hand controller used in the simulation was a three-axes control handle of the type that will be used in the Gemini spacecraft (fig. 9). Movements of the hand controller in the pitch direction (fore and aft) were about a pivot point located approximately half way up the handle. Banking maneuvers were performed by movements of the handle (right and left) about a pivot point at the base of the handle. Deadbands about the neutral position of the controller were $\pm 5^\circ$.

The torque characteristics of the hand controller are as follows:

<u>Maneuver</u>	<u>Break-out Force</u>	<u>Maximum Deflection</u>
Roll	3 in.-lb	9 in.-lb
Pitch	5 in.-lb	23 in.-lb

Spacecraft Display Panel.- The display panel presented to the pilot for the paraglider simulation consisted of Flight Director Attitude Indicator (FDAI), airspeed indicator, rate-of-descent indicator, altimeter, 24-hour clock, and various switches and lights. The display panel is shown in figure 10.

The vertical and horizontal needles on the face of the FDAI displayed the spacecraft yaw and pitch rates, respectively. The needle on the left side of the face indicated the spacecraft roll rate. Maximum deflection of the needles was 15 deg/sec.

The FDAI displayed the gimbal angles of the inertial platform and was aligned so that a zero reading about all three axes indicated that the vehicle was pointed north, level, and in a steady state glide condition. Motions of the rate needles and attitude indicator on the FDAI corresponded to a conventional aircraft "fly to" display. The

airspeed indicator provided a visual indication of spacecraft velocity during the simulation. The airspeed indicator used in the Gemini spacecraft is driven from a pitot source and therefore read indicated airspeed. The formula used in the simulation to correct for indicated airspeed was:

$$V_i = V_t \sqrt{\sigma}$$

TERMINAL LANDING SYSTEM SIMULATION

The simulation of the terminal landing system (TLS) consisted of the subsystems required to implement the guidance routine and operational procedures for terminal control and final approach. The simulation was accomplished completely within the analog computer room of the Guidance and Control Division. The only contact between the TLS operator located in the analog computer room and the pilot located in the simulator room was through the intercommunication system (fig. 16).

Guidance Routine

The guidance routine was based upon an impact predictor scheme which relates two parameters to the (TLS) operator: the vehicle's center of capability and the maximum available range about the center of capability. The center of capability is completely determined by the wind profiles and the vehicle's rate of descent.

Wind Profiles.- Wind profiles (fig. 11) in the X_e and Y_e direction were obtained for the vicinity of Ellington Air Force Base as a function of altitude for both the winter and summer months. The simulation had the capability of changing the wind profiles for different runs. The wind profiles used in the simulation were programed on diode-function generators. The wind profiles used in the equations of motion and vehicle simulation were (W_x, W_y) . Another wind profile (W_{x_p}, W_{y_p}) ,

which was some percentage change from the wind profile used in the vehicle simulation, represented the wind measurement that would be taken prior to the actual descent of the vehicle. This wind profile was used in the TLS simulation to calculate the vehicle's center of capability. The percentage difference between the vehicle's wind profile and the measured wind profile would depend upon the time between the last high altitude wind measurement and the actual descent of the vehicle.

Center of Capability.- The wind profiles (W_{x_p} , W_{y_p}) were repeatedly integrated from the vehicle's present altitude to the ground to determine the vehicle drift. However, due to the higher rate of descent at higher altitudes, the area under the wind profile was weighted as a function of altitude. The rate of change of the weighting function was $(-6.3 \times 10^{-4} \frac{1}{ft})$. The values of the integrated wind profiles X_w and Y_w were the distance between the center of capability and vehicle radar position. For example, if the vehicle had a radar position of ($X_r = 4,200$ ft, $Y_r = 5,000$ ft) and the integrated wind profiles were ($X_w = 400$ ft and $Y_w = -300$ ft) then the center of the vehicles capability was ($X_p = 4,600$ ft, $Y_p = 4,700$ ft). The vehicle radar position varied from the actual position by an amount equal to the accuracy of the radar. The accuracy of the radar was assumed directly proportional to the distance of the vehicle from the radar location. This accuracy was simulated as follows:

$$\text{Distance from vehicle to target} = \Gamma = \left[(X_e - X_r)^2 + (Y_e - Y_r)^2 + (Z_e - Z_r)^2 \right]^{\frac{1}{2}}$$

$$\text{Radar accuracy constants} = C_1, C_2, C_3$$

$$\text{Radar position} = X_r = X_e + C_1\Gamma, Y_r = Y_e + C_2\Gamma, Z_r = Z_e + C_3\Gamma$$

Maximum Available Range.- The area about the center of capability that the vehicle could attain was called the maximum available range or "footprint". This area was a circle, the radius of which can be obtained from the following formula.

$$R = (h) L/D$$

where

R = radius of the circle

h = present altitude of the vehicle

L/D = lift to drag ratio of the vehicle

Figure 12 shows a plot of R as a function of h for the paraglider plus Gemini spacecraft. It should be noted that when the paraglider is deployed, the vehicle may be headed in an opposite direction from the target. Therefore, an initial 180° turn maneuver may be required to align the vehicle in the proper direction. The altitude lost during an

initial 180° turn maneuver is small compared to the initial altitude and therefore, the reduction in the area of capability is small. However, the equation for the radius of the circle of capability was reduced from $R = 3.65h$ to $R = 3.48h$ to account for an initial 180° turn.

Guidance.- The guidance used during terminal descent was extremely simple. Once the TLS operator had the center of capability and maximum available range about the center of capability, the pilot was instructed to maneuver the vehicle to a heading equal to the azimuth angle between the center of capability and the target, assuming the target was within the maximum available range of the vehicle. The equation for azimuth heading was:

$$A_t = \arctan - (X_T - X_P)/(Y_T - Y_P)$$

The pilot continued to fly the instructed heading until the center of capability coincided with the target point. At this time, a constant bank maneuver was flown until the final approach altitude was reached. The pilot was then given instructions to enable him to attain the final approach glide path.

Displays

There were two display areas available for the TLS operator. The first area, which was used through out the study, consisted of existing analog X-Y plotting equipment. The second area, which was evaluated during the latter phase of the study, was a commercially available display system which essentially unified the X-Y plotting equipment into a single display.

X-Y Plotters.- The X-Y plotters used in the terminal landing system simulation were one 30 in. by 30 in. double pen plotter and three 10 in. by 15 in. single pen plotters (fig. 13). The 30 in. by 30 in. X-Y plotter showed Ellington Air Force Base and surrounding area (fig. 14) with a scale of 1 in. = 10,000 ft. One pen traced the radar position of the vehicle (X_r, Y_r) while the second pen traced the center of capability of the vehicle (X_p, Y_p). The second pen had the capability of tracing out the maximum available range of the vehicle at any time. This was accomplished by the TLS operator operating a mechanical switch on the analog console. The operator also had the ability to shut down either of the pens at any time. The first of the small 10 in. by 15 in. plotters showed Ellington Air Force Base (fig. 15) with a scale of 1 in. = 1,000 ft. The pen on this plotter traced either the center of capability or the vehicle's radar position with the change being made by actuating a mechanical switch on the analog console. The second 10 in. by 15 in. X-Y plotter (fig. 16) showed a closeup of the desired

runway with a scale 1 in. = 1,000 ft which was superimposed over the same runway with a scale of 1 in. = 500 ft. The center of the runway was always located at the center of the plotter. The pen on this plotter also had the capability of tracing either the center of capability or the vehicle's radar position. The third 10 in. by 15 in. X-Y plotter, shown in figure 17, is an altitude (h) versus range (Γ) trace of the vehicle's radar position with a scale of 1 in. = 1,000 ft. Various precalculated glide paths were used depending upon the magnitude and direction of the winds at the desired runway.

Projection Display.- A projection display system leased from Ling-Temco-Vought (LTV) by the Philco corporation under the TLS design study contract was also used in the simulation. This display system consisted of a control panel shown in figure 18(a), a 15 in. by 15 in. viewing screen shown in figure 18(b), and various support equipment. The main components of the LTV display system were the reference projector and the plotting projector. The reference projector displayed the same static information as the X-Y plotting equipment such as Ellington Air Force Base and surrounding area (1 in. = 20,000 ft), Ellington Air Force Base (1 in. = 1,000 ft and 1 in. = 500 ft), and an altitude range plot with various final approach glide paths. This information was stored on slides and could be portrayed on the viewing screen by setting the slide-selection-switch at the desired position. Two slides could also be displayed simultaneously if desired (fig. 18(b)).

The plotting projector traced out the movement of the vehicle or the center of capability in the same manner as the pen on the X-Y plotter. Color filters were also available and various colors were assigned and changed as desired.

Additional Information.- The only additional instrument information presented to the TLS operator was radar altitude and predicted heading (azimuth angle between the vehicle's center of capability and the target). This information was shown to the TLS operator by two circular dial type instruments as shown in figure 19. The operator also had at his disposal various plots such as: measured wind profiles, changing tendency of winds during a given period before the descent, frequency of wind gusts and their approximate magnitude, L/D versus stick position, and contingency landing site data.

TEST PROCEDURES

General

Wind profiles for both the vehicle and the guidance routine were selected and programed on diode-function generators. A runway and an approach direction were selected depending upon the wind profile. The center of the runway was designated as the target and was given the coordinates of ($X_T = 0, Y_T = 0$). A final approach glide path was selected along with initial vehicle position, direction of flight, and radar accuracies (C_1, C_2, C_3). The simulations were started at an altitude of 40,000 feet with the vehicle in a steady-state glide condition and the paraglider fully deployed. The initial conditions were:

$$h = 40,000 \text{ ft}$$

$$\gamma = -15.7 \text{ deg}$$

$$V_t = 155 \text{ fps (no winds)}$$

$$u = 137.5 \text{ (no winds)}$$

$$v = 0 \text{ (no winds)}$$

$$w = 71.6 \text{ (no winds)}$$

$$\alpha_k = 27.5 \text{ deg}$$

$$L/D = 3.56$$

$$\theta = 11.8$$

$$\Psi, \phi, p, q, r, \alpha_t, \Delta = 0$$

Recorded Data

The data recorded for each flight were:

X-Y Plotters With Vehicle Trace.-

Ellington Air Force Base and surrounding area (1 in. = 1,000 ft)

Ellington Air Force Base (1 in. = 1,000 ft)

Desired runway (1 in. = 1,000 ft and 1 in. = 500 ft)

Altitude versus range (1 in. = 1,000 ft)

Eight Channel Recorder (A).-

α_k	Keel angle of attack, deg
β	Angle of sideslip, deg
$\bar{u}, \bar{v}, \bar{w}$	Vehicle velocities relative to air mass, ft/sec
V_t	Total relative velocity, ft/sec
\bar{q}	Dynamic pressure, lb/ft ²
\dot{h}	Rate of descent, ft/sec

Eight Channel Recorder (B).-

W_x	East-west component of wind, ft/sec
W_y	North-south component of wind, ft/sec
p	Vehicle angular velocity about X_b , rad/sec
q	Vehicle angular velocity about Y_b , rad/sec
r	Vehicle angular velocity about Z_b , rad/sec
Δ	Change in lateral shroud lines, in./in.
α_t	Commanded trim angle of attack, deg
f	Fuel, lb

TEST SCHEDULE

The test schedule was broken down into the following categories of flight variables and mission objectives:

1. Radar accuracies
2. Differences in wind profiles, wind magnitudes, vehicle wind and measured wind
3. Initial vehicle and target position
4. Effects of cross wind and wind gusts
5. System failures and alternate procedures
6. Automatic direction finder (ADF)

The category of tests (a) were made to determine the effects of radar accuracies. During these cases, radar accuracies (C_1, C_2, C_3) were varied from 0 to 2 percent. The vehicle wind profiles (W_x, W_y) were summer winds at Ellington Air Force Base. The difference between vehicle winds and measured winds (W_{x_p}, W_{y_p}) was a nominal wind drift of 10 percent over a 1 hour period. The other variable was initial vehicle position.

The category (b) tests were conducted to determine the effects of variations in vehicle winds a measured winds for various wind profiles. During these cases, the winds were varied from summer winds to winter winds with the wind drifts varied from 0 to 30 percent. The radar accuracies were held at a constant 1 percent. The other variable was initial vehicle position.

The test category (c) was performed to show the effects of initial center of capability and target positions. The tests were made with all flight variables at the nominal condition (radar error 1 percent, wind error 10 percent and summer winds) except center of capability and target positions which were varied from range 0 to 140,000 ft.

Test category (d) was to show the effects of crosswinds and wind gusts. Flight variables remained at their nominal condition, but the vehicle was landed on runways that produced up to 45 degree crosswinds. Arbitrary wind gusts were also incorporated up to 50 percent of the present winds.

Test category (e) was made to study the effects of system failures and alternate landing procedures. These runs included FDAI misalignment, loss of gyro, vehicle outside of capability circle, changing runways at low altitudes, intersection of glide slope at low altitudes, orbiting downwind and of runway to intersect glide slope, and establishing of various holding patterns.

Category (f) tests were to determine techniques to be followed in the event the pilot had to use an automatic direction finder (ADF) to locate the field.

The test cases discussed above are listed in table 1.

DETERMINATION OF VEHICLE PERFORMANCE AND NORMAL OPERATING PROCEDURES

Prior to the actual tests runs, it was necessary to obtain information relative to the Gemini-paraglider flight characteristics and to study various ground control approach techniques. This section of the report discusses the results of the preliminary studies.

Vehicle Performance

The simulated vehicle was flown with lateral shroud length settings of $\Delta = 0$, $\Delta = .02$, and $\Delta = .04$ to determine the performance and maneuvering capability of the assumed Gemini-paraglider configuration. In these runs, the vehicle was flown with constant lateral shroud length settings and under a zero wind condition. The results of these flights are presented in figures 20 through 23. Figure 20 is a plot of rate of descent versus altitude and figure 21 a plot of total velocity versus altitude for the three lateral shroud length settings. Figures 20 and 21 show that as the lateral shroud length settings are increased, the rate of descent and total velocity for a given altitude increase at an increasing rate. Figure 22 shows turn rate versus altitude for lateral shroud length setting of $\Delta = .02$ and $\Delta = .04$ and figure 23 shows turn radius versus altitude for the same shroud length settings. Figures 22 and 23 indicate that as the lateral shroud length settings are changed, or the control handle is moved to the right or left, the turn rate increases proportionately and turn radius decreases proportionately. This proportionality seems to be approximately a direct function of shroud line length. Therefore, if a turn maneuver is required, half stick deflection ($\Delta = .02$) will produce a turn which is approximately twice as large as the turn with full deflection but with only a small increase in rate of descent and velocity (approximately 16 percent). This half standard rate turn is desirable for small maneuvers because the guidance routine is based upon the rate of descent during a steady state glide. When a large maneuver or a holding pattern is required, the standard rate turn or full stick deflection ($\Delta = .04$) is more desirable because of the higher turning rate. However, the (TLS) operator must consider the increased rate of descent and velocity (approximately 70 percent) resulting from such a maneuver.

Normal Operating Procedures

The preliminary studies indicated that a standard approach to the field and a spiral down holding pattern worked quite well during normal descents. The TLS operator referred first to the display of Ellington Air Force Base and surrounding area (fig. 14). When the vehicle's radar position and center of capability position had been established, the operator determined the maximum available range of the vehicle. If the target was within the maximum available range, the operator read the azimuth angle between the center of capability and the target and instructed the pilot to fly this heading on the FDAI. The pilot continued to fly the instructed heading until the center of capability coincided with the target. The azimuth heading changed from time to time during the descent, but due to the time involved for a single descent (approximately 20 minutes), the operator relayed this information to the pilot without difficulty. Once the center of capability coincided with target, the pilot was instructed to hold a constant hard over left bank angle until the final approach altitude was reached (approximately 5,000 ft). At this time, the operator looked at the display of the desired runway (fig. 16) and directed the pilot to fly a downwind leg heading which moved the center of capability point parallel to and about 1,000 feet to the right of the runway. The pilot continued to fly the downwind leg until the vehicle's position passed through a line parallel to the final approach glide path shown on the altitude versus range display, (fig. 17). This line was precalculated and allowed the pilot to make a 180 degree turn toward the desired runway and coincide with the desired glide path. This 180 degree turn maneuver placed the center of capability (or the vehicle's position) near the center line of the runway moving toward the target. At this time, the pilot was continuously instructed to make small corrections to maintain the proper heading until touchdown. The pre-flare and the flare maneuvers were not attempted during this simulation because of the lack of appropriate pilot displays.

The following assumptions were made for a normal descent:

1. Target was well within the area of capability
2. Summer wind profile
3. Wind error of 10 percent
4. Radar error of 1 percent
5. Glide path was based upon the measured wind
6. Runway was in the approximate direction of the surface wind

7. All instruments operational
8. The FDAI indicated true heading information

The ground trace of the vehicle as it approaches the field, orbits the runway, rolls out on downwind leg, does the 180° turn, and touches down for test run A-2 (normal) is shown in figure 24. The altitude versus range trace, including calculated glide path, upper and lower limits, and the point to begin the 180° turn maneuver toward the desired runway, is shown in figure 25. Time histories of various flight parameters during the descent are shown in figure 26. It should be noted that the precalculated glide slope and 180° turn maneuvers line were generated by the analog computer. However, prior to an actual descent, this information must be generated by the TLS computer.

RESULTS AND DISCUSSION

After the vehicle performance characteristics and normal operating procedures were determined, the test cases summarized in table 2 were conducted and recorded. The results of these cases are categorized in accordance with the test schedule and are presented in the following sections.

Radar Accuracies

Test cases A-1 through A-5 were conducted to determine the effects of radar accuracies. Normal radar accuracies are in the order of $\pm 1^\circ$ in elevation and azimuth angle. At maximum available range of 140,000 ft and deployment altitude of 40,000 ft, the possible position discrepancy would be approximately $\pm 2,800$ ft due to range error and ± 800 ft due to elevation error. Because the equations-of-motion were written using an earth fixed orthogonal coordinate system, it would have been difficult to incorporate the radar error as a function of elevation and azimuth angle. Therefore, percent errors (C_1, C_2, C_3) were added or subtracted to each of the spacecraft position axes (X_e, Y_e, Z_e). For example, if the radar at the target site had the coordinates ($X_e = 0, Y_e = 0$), and the spacecraft has the position of ($X_e = 140,000$ ft, $Y_e = 0, Z_e = -40,000$ ft), and the radar accuracies were set at ($C_1 = C_2 = C_3 = 2$ percent), there would be a radar error of $\pm 2,800$ ft in range and 800 ft in elevation.

The test cases A-1 through A-5 were relatively nominal cases using summer wind profiles and 10 percent wind errors. The initial position

was changed for each case and the radar accuracies were varied from 0 percent to 2 percent. The results of these cases indicated that as long as the radar site was at the same location as the landing site, radar accuracies in the order of 2 percent had no noticeable effect on the success of the guided descents. In each case, the TLS operator was able to follow the normal procedure and guide the vehicle to the center of the desired runway. The only time that radar accuracies may become relevant is when the radar is located at the primary landing sites and the vehicle must be guided to a contingency landing site some distance away. The remainder of the test cases were run with radar accuracies of 1 percent.

Wind Effects

General.- Test cases B-1 through B-14 were run to determine the effects of wind on the terminal descent of the Gemini-paraglider earth landing system. During these cases, both summer winds (figure 11(a)) and winter winds (fig. 11(b)) including gusts, were utilized. The wind error between measured wind and vehicle wind was varied up to 30 percent for both wind profiles. Radar accuracies were held constant at 1 percent. The only other variable during these tests was initial spacecraft position. Wind profiles and wind gust information were obtained from references 5 and 6.

Summer Wind.- All cases with summer winds (B-1 through B-6) were completed successfully (runs terminating on the runway). The 30 percent error between the measured wind profile and the vehicle wind profile presented no significant guidance problems and the TLS operator simply followed the normal procedure during this series of runs. The summer wind near the ground of approximately 20 ft/sec and the wind error of 30 percent were not sufficient to produce an accumulated error large enough to cause the vehicle to miss the length of runway. This can be seen in figure 27, where miss distance is plotted against altitude at intersection of glide slope. The wind gusts encountered in runs B-2, B-4, and B-6 were not of a sufficient magnitude to seriously deteriorate the spacecraft performance. The gusts did excite some short period oscillations, but in most cases the pilot concentrated on holding the heading and relied upon the inherent stability of the vehicle to damp the oscillations. Except for occasional small heading corrections during final approach, the TLS operator was usually unaware that the spacecraft had even experienced a gust.

Winter Wind.- In the cases using winter winds (B-7 through B-14), the wind profiles and wind gusts had a significant effect upon both the guidance problem and the performance of the spacecraft. Upon deployment of the paraglider (start of the simulated runs), the TLS operator displayed both the vehicle position and the center of capability. Because of the magnitude of the winter wind profiles, these quantities

were as much as 70,000 ft apart and, depending on the location of the target, could even be on opposite sides of the landing site. When this type of situation occurred, the pilot would actually be instructed to head the spacecraft away from the landing site. For example, if the vehicle position was $X_e = 30,000$ ft east and the center of capability was $X_e = 30,000$ ft west, the predicted heading would be 90° (east), which is directly away from the target. However, as long as the TLS operator based his instructions to the pilot on the center of capability and not on the vehicle position, he was able to guide the spacecraft to the landing site. When the TLS operator attempted to guide the vehicle to the final approach position, the percent error between measured and vehicle winds became critical. If the vehicle intersected the precalculated glide slope at 5,000 ft and there was a 30 percent error in the wind, the vehicle would miss the center of the runway by 3,000 ft and possibly miss the entire runway (fig. 27). The reason for the larger miss distances encountered when winter winds were used is that the vehicle glide slope is much steeper. A given percent error in measured winter winds would produce a much larger miss distance at touchdown than the same percent error in summer winds (fig. 25). Assuming that the TLS operator was aware of the wind error, he would guide the spacecraft to intersect the glide slope at a lower altitude, (i.e. 3,000 ft), thereby reducing the miss distance to 1,650 ft, thus causing touchdown on the runway. As long as there were no wind gusts and the TLS operator followed the above procedures, he was able to successfully guide the spacecraft to touchdown the desired runway; of course, the desired runway had to be in the direction of the surface wind (cases B-7 through B-10). When severe wind gusts in the order of ± 30 ft/sec were incorporated in the descents, the spacecraft motions became quite large and the pilot had difficulty holding a precise heading. Also, when gusts normal to the runway were encountered on final approach, the vehicle would translate to one side and abrupt heading correction were required. If these gusts were experienced above 1,000 ft, the pilot and the TLS operator could correct for the disturbances and land the spacecraft on the desired runway. However, severe gusts below 1,000 ft caused such large spacecraft motions that it was extremely difficult, and at times impossible, to land the spacecraft on the runway. It should be noted, however, that this was not a limitation of the Terminal Landing Facility, but rather a flight characteristic of the paraglider earth landing system which is known to have control problems in the presence of gusty winds. Also, gust magnitudes of ± 30 ft/sec below 1,000 ft can only be encountered in tropical storms or thunderstorm activity. For airfields located in Texas, statistical data indicate that the probability of encountering such conditions is less than 0.5 percent during daylight hours. In any event, if these conditions are forecasted for the primary landing site, the spacecraft should be landed at an alternate site.

Wind Gusts. - The wind gusts used in some of the test cases were completely arbitrary in number and direction and were incorporated into the vehicle wind profiles (W_x, W_y) in either the positive or negative direction by means of several switches on the analog console. All gusts were assumed to have a wedge shape profile with a 2 second time interval for each side of the wedge. The magnitude at the peak of the gusts was 1.5 times that of the magnitude of the ground winds at the time of the gusts. For example, if a gust was encountered and the wind at the landing site was 30 ft/sec, the wind magnitude at the peak of the gusts varied from 15 ft/sec to 45 ft/sec depending on the direction of the gust. If the gust encountered was normal to the vehicle wind profile, the total wind magnitude at the peak of the gust was 33.5 ft/sec and the wind direction changed 26.6°.

Landing Site Offset. - The integration of the measured profiles (W_{x_p}, W_{y_p}) represents the distance the vehicle will drift during descent. This drift should be accounted for prior to deployment of the paraglider. That is, the actual landing site should be off-set by the amount of the integrated wind profiles (X_w, Y_w). For example, if the paraglider is deployed at an altitude of 40,000 ft directly over the target, the wind profile may be of a sufficient magnitude (larger than the forward velocity of the vehicle) to prevent the spacecraft from reaching the target. Therefore, after each wind measurement, the wind profiles and integrated wind profiles should be transmitted to the Integrated Mission Control Center so that the landing site off-set can be incorporated into the reentry guidance system.

Initial Position

It has been stated that under normal conditions there is no particular control problem as long as the target is well within the area of capability. Cases C-1 through C-9 were conducted to determine the effects of target location on or near the edge of the area of capability. These runs were started with the vehicle heading away from the target and therefore an initial 180° turn was required to place the spacecraft on course. The area of capability, as noted previously, had been reduced to allow for an initial 180° turn. However, even under ideal conditions (radar error = 0, wind error = 0), the 180° turn had to be performed immediately after complete paraglider deployment for the vehicle to reach the edge of the area of capability. Therefore, the pilot should have the initial predicted heading prior to paraglider deployment. In an actual flight, a very close approximation to the correct heading can be made prior to paraglider deployment by obtaining a radar position at an altitude above complete paraglider deployment (i.e. 50,000). Then, assuming that this earth position (X_e, Y_e) would

be the same at an altitude of 40,000 ft (full paraglider deployment), the drift due to the measured wind can be added to the earth position. This corrected point would be very close to the true center of capability at paraglider deployment and could be used for computing an initial predicted heading. The use of this technique would eliminate the time wasted between paraglider deployment and the time it requires the TLS operator to provide the pilot with the initial predicted heading.

When the landing site was on or very close to the edge of the initial area of capability, the percent error in the winds became very important. If the percent error was in the direction of flight, the spacecraft could make the field with sufficient altitude to turn and land on the desired runway. However, if the percent error was not in the direction of flight, the spacecraft failed to reach the desired runway and at best, landed at a closer runway or on the apron of the field. In any event, these cases were marginal and the TLS operator first looked for a contingency landing site in the area of capability. If there was not a contingency landing site available, the TLS operator intermittently displayed the area of capability to detect an increase or decrease in the measured winds. When the edge of the area of capability moved in a direction to encircle more of the primary site, there was an increase in winds in the direction of flight and the chances of reaching the field were good. When the edge of the area of capability moved so that it did not encircle the target, the flight was aborted. It should also be noted that in the event the spacecraft did reach the field, it was approaching at a very low altitude and the TLS operator was required to direct the spacecraft over an area where there were no local obstacles. The display of Ellington Air Force Base (fig. 15) was very useful for this purpose.

Cross Wind

Summer Cross Wind. - Cases D-1 and D-2 were run to determine the effects of summer cross winds. Wind gusts of up to ± 50 percent of the ground winds were used. The vehicle was landed on a runway that had up to 45° cross winds. All other flight variables remained at their nominal conditions. The results of these tests indicated that there was no particular control problem. The TLS operator estimated the crab angle (angle between light of flight and spacecraft heading) and directed the pilot to fly this angle with respect to the desired runway. Small deviations from this angle were then made in the same manner as a normal flight.

Winter Cross Wind. - Winter cross winds were not investigated in the study. However, in the event that they are encountered, the TLS operator would select a runway nearest to the wind direction. The maximum angle between the runways used in the simulation was approximately 90° and thus even if the TLS operator selects the nearest runway, the

crosswind could be as much as 45° . Here again, the TLS operator would estimate a crab angle and direct the pilot to fly this angle with respect to the desired runway. Because of the magnitude of the winds, the crab angle will be quite large and will affect the spacecraft velocity in the plane of the runway. For example, if the surface wind was 35 ft/sec and the selected runway was at a 45° angle to the wind, the spacecraft would have to crab approximately 24° (assuming air speed velocity of 60 ft/sec at touchdown). This would reduce the relative forward velocity in the plane of the runway to approximately 55 ft/sec. Due to this reduction in relative velocity, the altitude at which the spacecraft intersects the precalculated glide slope should be lower than normal (i.e. 3,000 ft). It should be noted that the crab angle of the spacecraft does produce some lateral component of velocity but if the crab angle is correct, the lateral velocity will never exceed the maximum design loads of the landing gear of 30 ft/sec (assuming the winds never exceed the relative velocity of the spacecraft). The above example of a 35 ft/sec and 45° crosswind produces the maximum lateral spacecraft velocity of approximately 12.3 ft/sec.

System Failures and Alternate Procedures

General.- Although the normal procedures work quite well under nominal descent conditions, there are some instances where alternate procedures should be used. Runs E-1 through E-18 include some of the system failures that might occur during a Gemini-paraglider terminal descent and the alternate procedures that could be used. In addition, some procedures other than the nominal were evaluated to determine their feasibility under certain conditions.

No Heading Information, All Turns Relative.- During a paraglider descent, the FDAI will continuously display roll, pitch, and yaw attitudes with respect to the local earth vertical and orbital plane. The ground support tracking system and associated displays will be all referenced to true North. This incompatibility between the pilot's heading indicator and the true earth heading of the vehicle was resolved in the simulation as follows: The ground controller traced the spacecraft center of capability with the spacecraft in a steady state glide to determine the spacecraft actual heading. The difference between predicted heading and actual spacecraft heading was computed and relayed to the spacecraft in terms of degrees to turn right or turn left from his present heading. The pilot made use of the FDAI to turn the exact number of degrees, thus moving the center of capability toward the target. Once the center of capability was moving toward the target, the pilot relayed to the TLS operator the heading indication displayed on the FDAI. With this information, the TLS operator determined the discrepancy between actual spacecraft heading and indicated heading, then biased commands to the pilot by this amount.

During run E-1, no difficulty in guidance was experienced once the FDAI discrepancy was determined. However, a degradation in performance occurred due to the time needed to trace the center of capability long enough to establish the spacecraft heading. This degradation in performance could have been eliminated by either having the pilot manually bias the FDAI from the orbital plane to true north or by having the ground support equipment biased by this amount. This should be a fairly simple procedure, since the angle between the orbital plane and true north would be a known quantity at this time.

No Gyro Approach, Start and Stop All Turns.- The possibility of a FDAI failure cannot be ignored. Should this failure occur, both attitude and heading information would be lost to the pilot. Therefore, the pilot cannot immediately attain the initial predicted heading. The TLS controller must wait a short time to establish a spacecraft heading (trace of the center of capability). Once the heading is established, the controller can issue "start and stop turn" instructions to the pilot in order to turn the spacecraft to the proper heading. Another problem associated with this condition is that display information does not immediately reflect the actions of the spacecraft. This lag, which occurs to both "distant" and "close in" controlling, complicates the controller's task. It should also be noted that during a steady state glide the Gemini-paraglider is at approximately maximum L/D and has static and dynamic stability about all three body axes. Therefore, under normal wind conditions the pilot need only to actuate the hand controller in roll to perform turn maneuvers.

In run E-2 (no gyro approach), the spacecraft was brought over the field at an altitude sufficient to allow a descending spiral to be initiated. Once the proper altitude was reached, the spacecraft was directed to a safe landing using the "start and stop" method of heading control (roll control only). One difficulty encountered on the turn to final approach was that an overshoot of approximately 40° occurred due to the lag between display and spacecraft action. This situation might be avoided by commanding half or quarter standard rate turns, but this type of turn must be initiated before the trace of the spacecraft crosses the 180° turn line of the altitude versus range plot. The problem in heading control decreased in direct proportion to the amount of heading change required, and at no time during the run did heading control pose an impossible task. In an actual paraglider descent, the pilot would probably have the field in sight and would be able to avoid overshoot problems of this type.

Orbit Center of Field and Intersect Glide Slope at Low Altitudes.- One of the problems the ground controller encounters during final approach is to determine at what altitude the glide path should be intersected. The advantage associated with intersecting the glide path at high altitudes (6,000 to 8,000 feet) is that it allows for a longer

interval of time on the final approach heading, thus enabling the TLS operator to ascertain the drift due to any crosswind component and more precisely line up the spacecraft with the runway. The disadvantage of this procedure is related to the accuracy of the assumed winds during the final approach. The glide corridor shown on the profile display is a function of the vehicle's L/D and the magnitude of the measured wind component in the landing plane. Therefore, the displayed glide path will be in error by the amount of wind change since the last measurement. Assuming that the desired landing point is located in the center of the runway, a 20 percent error between measured winter winds and vehicle winds corresponds to a miss distance approximately 2,430 ft from an altitude of 6,000 ft, and only a miss distance of approximately 700 ft from an altitude of 2,000 ft to the ground (fig. 27).

It was determined that the advantages associated with intersecting the glide path at low altitudes far outweighed the loss of time available for line up with the runway. The series of runs (E-3 through E-5) dealing with intersecting the glide corridor at altitudes down to 2,000 ft fully demonstrated the feasibility of this procedure. All runs terminated on the runway and within 1,200 ft from the center of the runway.

Change Wind and Runway at Low Altitude. - During final approach, a condition may develop which requires a change of landing runway. Of particular concern was the determination of that point in the flight at which a runway change could be made without seriously jeopardizing the landing operation. To determine the ability of the ground controller to react to a sudden runway change while planning an approach to another runway, several runs were made in which the wind and runway were changed by 90° to 180° (runs E-6 through E-9). The altitude of the spacecraft at the time of the change varied from 8,000 ft to 3,000 ft. Analysis of these runs established a lower limit of 3,000 ft as the altitude at which the spacecraft was committed to land on a given runway.

Orbit Downwind End of Runway to Intersect Glide Slope at Low Altitude. - This series of runs (E-10 through E-12) was in many respects similar to runs (E-3 through E-5). The primary difference between the two series was the position of the orbiting spiral. In these runs, the spiral pattern was controlled to remain as close as possible to the downwind end of the runway, which eliminated the downwind leg of descent. Therefore, the TLS operator did not have the use of the line on the profile display which indicated the time to perform the 180° turn maneuver toward the runway. When this procedure was used, the spacecraft must remain in a spiral pattern until the descent was very close to the glide slope. At this time, the TLS operator relayed an inboard runway heading to the pilot. During these runs, the glide slope intersection varied from 1,200 ft to 2,000 ft. No difficulty in controlling the vehicle was encountered in the runs and, because of the very low altitude

used for glide slope intersection, all landings terminated on the runway. Because there is some difficulty in acquiring the correct glide slope this procedure should not be used to intersect the glide slope at high altitudes. Due to the elimination of the downwind leg of the descent and the possible improved pilot view of the runway, this procedure might be used at contingency or emergency landing sites where there is no glide slope information.

Establish Same Holding Pattern Regardless of Winds. - In test cases E-13 and E-14, three holding patterns were investigated to determine their application and feasibility as an alternate procedure to the spiral down technique. When the spiral down technique is used in the presence of wind, the vehicle drifts and the spiral pattern progresses in the direction of the wind (fig. 24). It is not a particularly difficult task to compensate for this effect since it is a simple matter to roll out on a heading which will return the vehicle to the center of the runway. In addition, this direction of drift can be used to corroborate the measured wind profile. However, the condition may arise where the pilot or the TLS operator desired to hold the vehicle in a fixed pattern regardless of the winds. The three holding patterns studied were:

1. A simple box or rectangular pattern performed with 90° turn maneuvers.
2. A 90° - 270° maneuver performed with a 90° turn to the left and then a 270° turn to the right with a leg between the next 90° - 270° maneuver.
3. A steady circular pattern performed by increasing or decreasing the rate of turn.

The first two maneuvers worked quite well as long as two sides of the box or the legs between 90° - 270° maneuvers were into or with the wind, but the third method did not work. It became almost impossible to hold a steady circular pattern in the presence of wind because of lag between action of the spacecraft and the vehicle trace. It should also be noted that holding patterns (1) and (2) use much more control fuel than the spiral holding pattern due to the almost continuous maneuvering required.

Control System With Rate Command in Roll. - In test case E-15, the roll control mode was changed for attitude command to a constant rate command. Therefore, if the stick was moved to the right or left past the $\pm .5^\circ$ deadband about the neutral position (upright position), the lateral shroud lines would lengthen or shorten at a rate of 9 in./sec ($\dot{\Delta} = .02452$ (in./in.)/sec). The lines would continue to change at this rate until the stick was returned to the neutral position, or until the

limits of the lines were reached ($\Delta = \pm .04$ in./in.). This change in control mode eliminated the necessity of the pilot to "hold in" a commanded bank angle with the control handle. With the roll control in rate command, the pilot deflected the control handle until the desired bank angle was reached and then returned the handle to the upright position. After the test case E-15 was run with rate command in roll the same case was run again (E-16) with the roll control back in the attitude command mode. The two cases were then compared with regards to handling qualities and fuel consumption. The results of the comparison indicated that the rate command mode was more sensitive than the attitude command. This was caused by roll position overshoots in the rate command mode, almost certainly due to pilot overcontrol. When the pilot attempted to hold a constant heading or return the spacecraft to a steady state glide, the tendency was to overshoot the desired heading and thus the pilot was required to manipulate the control handle back and forth until the correct heading was attained. This tendency to overshoot a bank angle position did not make the spacecraft uncontrollable, but it did add to the pilot-TLS operator control problem. There was, however, a saving in control fuel in the rate command mode over the attitude command. This may have been caused by the continuous corrections required to maintain a desired bank angle in attitude command mode, while in the rate command mode the pilot can return the hand controller to the neutral position once the desired bank angle is attained. The fuel consumed for the two runs, not including the dive and flair maneuvers, were 3.24 lbs for E-15 (rate command) and 5.26 lbs for E-16 (attitude command). The assumption used in the test cases were that the consumption rate in pitch was .236 lb/sec (while the pitch winch was operating), the consumption rate in roll was .105 lb/sec (while the roll winch was operating), and the leakage rate was constant at .1 lb/min. It should be noted that two test runs are not conclusive evidence to state that there will be a saving of fuel in all cases.

Varying Turn Rate Maneuvers. - In test cases E-17 and E-18, all turn maneuvers were performed with half and quarter standard rate turns, respectively. To perform a half or a quarter standard rate turn, the stick was simply deflected half or quarter of full deflection (fig. 22). These runs were performed successfully and with very little degradation of performance during the descents. However, when a 180° turn maneuver to final was performed with a turn rate less than standard, it was initiated sooner and at a further distance from the runway. Also, if the winds are strong, and a less than standard rate turn is performed, there may be considerable drift due to the extended time required to make the turn. Thus, if the winds are strong during final approach, all turn maneuvers should be performed with standard rate turns.

Automatic Direction Finding (ADF)

General.- There is a possibility that the spacecraft may land at sites other than those with the proper ground support equipment. For this eventuality, a navigation aid aboard the spacecraft could enhance the probability of performing a successful landing at a contingency or emergency field. Although there are many types of navigation aids and onboard displays that could be used, consideration was given only to a low frequency receiver which provided bearing information. With this type of system onboard, descents were made (cases F-1 through F-6) to determine the feasibility of using ADF equipment during a contingency or emergency landing.

Test Conditions.- The low frequency transmitter was located at various points in the vicinity of the landing site, ranging from a point in the center of the runway to one nautical mile from the approach end and in line with the landing runway. Relative bearing from the spacecraft to the station was displayed to the pilot by a circular heading instrument (much the same as the predicted heading shown in fig. 19). The initial conditions were such that the spacecraft was always positioned within maneuvering range of the station. Also, the spacecraft altitude at station passage was such that maneuvers about the station could be performed. Surface wind at the landing site and the breakout altitude (time the spacecraft must leave the station inbound to the field) were given to the pilot prior to the run. Since there was no method available to simulate the pilot's visual contact with the field, the ground controller provided lineup information after the spacecraft passed over the station inbound to the field.

Results.- Under the somewhat unrealistic conditions used in the ADF simulation, the descents were successfully terminated near the center of the runway. However, it should be noted that during the simulation the pilot was given both surface wind and breakout altitude for each run. When an actual ADF descent is performed, the pilot will probably be in contact with the field and will obtain the surface wind from the tower. Thus, the pilot must determine without assistance, except for precalculated charts and the location of the low frequency transmitter, the breakout altitude. To determine this altitude, the pilot must assume the wind does not change direction or magnitude from the surface to the breakout altitude. During most descents the wind will not remain a constant and, therefore, if the wind variation is large and the transmitter is a considerable distance from the field, the possibility exists that the spacecraft may miss the runway. Also during the simulation, the pilot was directed to the desired runway. For an actual ADF descent, the pilot must be in visual contact with the field at the breakout altitude and maneuver the vehicle to the desired runway without the aid of the TLS. For these reasons, an ADF descent should not be attempted except as an emergency procedure.

Pilot Procedures.- If an ADF navigation aid is incorporated onboard the spacecraft and the situation arises where it must be utilized, the following information must be available and landing procedures used:

1. Information about various fields, such as data on beacon, runways, frequencies, and paraglider glide slopes versus head winds.
2. Altitude frequency of the beacon, approach charts, and glide slope data must be made ready for the particular field selected prior to retrofire.
3. After paraglider deployment, a standard corrective wind drift approach must be made to enter high cone.
4. A 90° - 270° procedure should be used during letdown.
5. The departure altitude for final approach determined from tower relayed winds.
6. The 90° - 270° turns altered (if necessary) so the spacecraft will be inbound at the selected altitude.
7. There must be visual contact with the duty runway at departure altitude from low cone.

Display Areas

X-Y Plotters.- The display area, consisting of existing analog equipment (fig. 13), had the distinct advantage that there was never any question as to the physical location of the quantity being displayed. That is, the pen always represented the present radar position or present center of capability of the vehicle. Thus, after a scale change, or at the beginning of a run, there was no time wasted waiting for a "blip" or a scribed line to appear on a viewing screen. However, there were many disadvantages associated with this display area, such as:

1. The display area was entirely too large.
2. Because of the size of the area, the TLS operator was required to physically move from one display to another.
3. During the final approach, the TLS operator could not view the glide slope and the pre-selected runway simultaneously.
4. The glide slope and/or the desired runway could not be changed during final approach.

5. The display would sometimes become cluttered and there was no method of clearing or erasing the displays during a flight.

Projection Display. - This display area, consisting of a commercially available projection display system (fig. 18(a)), had only one main disadvantage and that was that it was sometimes impossible to determine the exact location of the quantity being displayed. This occurred at the beginning of a test run, after a scale change, or after the viewing screen had been cleared. Subsequent to each of these operations, there was a short time interval before the function being displayed appeared on the viewing screen. This was extremely undesirable during the final approach due to the requirement for constant monitoring. However, there were a number of advantages associated with the display, such as:

1. The display area was fairly compact.
2. The TLS operator could display any stored slide or combination of slides on the viewing screen at any time without changing his position.
3. The TLS operator could display both the glide slope and pre-selected runway simultaneously (fig. 18(b)).
4. The glide slope and/or the pre-selected runway could be changed during final approach by means of the slide-selection-switch.
5. The display could be cleared at any time during the flight.
6. Various color overlays could be used to add clarity to the display.

Additional Displays. - The display showing radar altitude and predicted heading (fig. 19) was used in both display areas and was an essential part of the terminal landing facility.

It has already been stated that it is quite important that the TLS operator be aware of differences between measured winds and actual winds at the landing site. To accomplish this, two instruments should be incorporated in the finalized terminal landing system:

1. A dial type instrument showing measured and actual ground wind directions
2. A digital meter showing measured and actual ground wind magnitudes.

With this information, the TLS operator can take whatever action is required to intersect glide slope at normal altitude, intersect glide

slope at low altitude, change glide slope and/or change runways, et cetera. In addition, the TLS console should have a keyboard selection, of all the runways at the primary landing site and a keyboard selection of various precalculated glide paths for a range of constant head winds.

Computer Functions

The landing procedures evolved in this simulation require a TLS computer capable of performing the following functions:

1. Calculate and store wind profiles (W_{x_p} , W_{y_p}) directly from radar tracking information. The computer must have the ability to instantaneously update any portion of the stored wind information at any time.
2. Calculate the center of capability and area of capability from stored wind profiles. The calculation of the center of capability should not take longer than 5 seconds per calculation, and generation of the area of capability should not take longer than 4 seconds.
3. Calculate a glide slope and 180° turn line in the plane of the desired runway from known spacecraft velocity components and stored wind profiles. The time to generate a glide slope should not take longer than 3 seconds.
4. Drive the display system.

CONCLUDING REMARKS

Results of the analog simulation study may be summarized as follows:

1. If the primary landing site is within the area of capability of the spacecraft, a guidance routine based on the integration of measured wind profiles is feasible for control to the site.
2. High altitude wind measurements should be taken periodically throughout the orbital phase of the mission. However, the last high altitude measurement should be taken at the primary landing site as close to retrofire time as possible to minimize wind error. Continuous updating from altitudes of 0 to 5,000 ft should also be performed during reentry and paraglider modes.

3. After each wind measurement, wind profiles and integrated wind profiles should be transmitted to the Integrated Mission Control Center so that the landing site off-set can be incorporated into the reentry guidance system.
4. When summer winds with arbitrary gusts are encountered, normal operating procedures can be followed. Summer wind near the ground of approximately 20 ft/sec and wind errors of 30 percent will not cause the spacecraft to miss the runway. Wind gusts in the order of ± 10 to 15 ft/sec do not seriously deteriorate the performance of the spacecraft.
5. When strong winter winds are encountered, the TLS operator must base instructions to the pilot on the center of capability. If there is a large wind error, the spacecraft must intersect the glide slope at a low altitude. When tropical storms or thunderstorms activity is predicted for the primary landing site, the spacecraft should be landed at an alternate site due to the vehicle flight limitations.
6. If winter crosswinds are encountered, a large spacecraft crab angle will be required to counteract the crosswind which in turn produces a lateral component of velocity. However, if the crab angle is correct, the lateral velocity will never exceed the maximum design loads of the landing gear.
7. Two additional instruments would aid the TLS operator in detecting changes in surface winds; these are:
 - a. A dial type instrument showing measured and actual wind direction, and
 - b. A digital meter showing measured and actual ground wind magnitudes.

In addition, the TLS console should have a keyboard selection of all the runways at the primary landing site and a keyboard selection of various precalculated glide slopes for a range of constant head winds.

8. During final approach, the spacecraft cannot change landing runways below 3,000 ft without seriously jeopardizing the landing operation.
9. As long as the radar equipment is at the landing site, normal radar accuracies in the order of $\pm 1^\circ$ in azimuth and elevation angles have no noticeable effect on the success of the controlled descents. However, radar accuracies may become relevant

if the radar is located at the primary landing site and the spacecraft must be guided to a contingency landing site some distance away.

10. A calculated initial predicted heading based on the vehicle's position prior to complete paraglider deployment should be transmitted to the pilot during paraglider deployment.
11. When the initial target position is near the edge of the area of capability, the TLS operator should control the spacecraft to a contingency landing site near the center of capability. If there is no such contingency landing site, the TLS operator should monitor the area of capability to determine if the flight should be aborted.
12. Additional navigation aids aboard the spacecraft could increase the probability of performing a successful landing if the spacecraft is required to landing at sites other than those with the proper ground support equipment. A low frequency transmitter located in the vicinity of the landing site appears to show promise; however, additional studies are required to verify this hypothesis.
13. The discrepancy between actual spacecraft heading and pilot's indicated heading should be eliminated by either having the pilot manually bias the FDAI from the orbital plane to true north, or have the ground support equipment biased by this amount.
14. A FDAI failure does not constitute an abort as long as two-way communications exist since the TLS operator can direct the spacecraft to the landing site by means of the "start and stop turn" method of heading control.
15. A projection type display system has the following advantages over the display utilizing existing analog computer recording instruments:
 - a. The display area was compact.
 - b. The TLS operator could display any stored slide or combination of slides on the viewing screen at any time, and therefore did not have to change position.
 - c. The TLS operator could display both the glide slope and preselected runway simultaneously.

- d. The glide slope and/or the preselected runway could be changed during final approach by means of the slide-selection-switch.
 - e. The display could be cleared at any time during the flight.
 - f. Various color overlays could be used to add clarity to the display.
16. Some of the functions that a TLS computer must perform are:
- a. Calculate and store wind profiles directly from radar tracking information and have the ability to instantaneously up-date any portion of the stored wind information at any time.
 - b. Calculate center-of-capability and area of capability from stored wind profiles. The calculation of the center of capability should not take longer than 5 seconds per calculation and the generation of the area of capability should take no longer than 4 seconds.
 - c. Calculate a glide slope and 180° turn line in the plane of the desired runway from known spacecraft velocity components and stored wind profiles. The time to generate a glide slope and 180° turn line should not exceed 3 seconds.
 - d. Drive the display system.

REFERENCES

1. Gemini Spacecraft Crew Station System Specification, McDonnell Aircraft Corporation, January 15, 1963.
2. Internal Letter PFS/63-131, Longitudinal Rigging Analysis for the Gemini Prototype Wing, North American Aviation, Inc., July 29, 1963.
3. Report SID 63-768, Test and Model Information for the Half-Scale Paraglider Wing and Capsule in the Ames 40 by 80-Foot Wind Tunnel, North American Aviation, Inc., June 21, 1963.
4. Report SID 62-1141, Aerodynamic and Loads Data Derived From Wind Tunnel Tests of the Half-Scale Gemini Paraglider/Capsule Flight Vehicle in the Ames 40 by 80-Foot Wind Tunnel, North American Aviation, Inc., September 15, 1962.
5. Internal Letter FS/62-149, Lateral Dynamic Analysis of the Gemini-Paraglider Recovery System, North American Aviation, Inc., July 9, 1962.
6. Terminal Operations of the Gemini paraglider, Landing and Recovery Division, Manned Spacecraft Center, June 3, 1963.
7. The Use of Upper-Air Winds for Guiding Spacecraft Descent, Space-flight Meteorology Group, U. S. Weather Bureau, September 20, 1963.
8. Wind data for MSC Little Joe II Launch Vehicle Studies, White Sands Missile Range, October 15, 1962.
9. Notes on Space Technology, Langley Aeronautical Laboratory, February-May 1958.

APPENDIX A

EQUATIONS OF MOTION

A careful analysis of the physical problems involved in the desired simulation usually reveals that a number of simplifications can be made to reduce the task of programming the complete equations of motion. The equations described herein are applicable to the Gemini capsule plus paraglider earth landing system and incorporate the following assumptions:

- (1) The vehicle has mirror symmetry about the X_b - X_b plane.
- (2) The vehicle has mirror mass distribution about the X_b - Y_b plane. (Products of inertia I_{xy} and I_{yz} and zero.)
- (3) The earth's gravitational field is constant.
- (4) The earth model is flat and non-rotating.
- (5) Atmospheric density is a function of altitude only.
- (6) The vehicle is a rigid body.

The derivation of the equations of motion may be found in reference 9 and have therefore been compiled without derivation.

EQUATIONS OF MOTION

Force Equations

$$\dot{u} = rv - qw + \frac{X_a}{m} - g \sin \theta$$

$$\dot{v} = pw - ru + \frac{Y_a}{m} + g \sin \phi \cos \theta$$

$$\dot{w} = qu - pv + \frac{Z_a}{m} + g \cos \phi \cos \theta$$

Moment Equations

$$\dot{p} = \left(\frac{I_y - I_z}{I_x} \right) qr + \frac{I_{xz}}{I_x} (\dot{r} + pq) + \left(C_{z\Delta} + C_{z\beta} + \frac{C_{z\rho d}}{2 V_t} \right) \frac{\bar{q}}{I_x} Sd$$

$$q = \left(\frac{I_z - I_x}{I_y} \right) pr + \frac{I_{xz}}{I_y} (r^2 - p^2) \left[C_{m\alpha} (\alpha_k - \alpha_t) + \frac{C_{mqd}}{2 V_t} \right] \frac{\bar{q}}{I_y} Sd$$

$$\dot{r} = \left(\frac{I_x - I_y}{I_z} \right) pq - \frac{I_{xz}}{I_z} rq + \frac{I_{xz}}{I_z} \dot{p} \left(C_{n\beta} + C_{n\Delta} + \frac{C_{nr d}}{2 V_t} \right) \frac{\bar{q}}{I_z} Sd$$

Aerodynamic Forces

$$X_a = C_x \bar{q} S$$

$$Y_a = \left(C_{y\beta} + C_{y\Delta} \right) \bar{q} S$$

$$Z_a = C_z \bar{q} S$$

Vehicle Attitude Angles

$$\dot{\psi} = \frac{q \sin \phi + r \cos \phi}{\cos \theta}$$

$$\dot{\theta} = q \cos \phi - r \sin \phi$$

$$\dot{\phi} = \rho + \dot{\psi} \sin \theta$$

Velocities With Respect to Air Mass

$$\bar{u} = u - W_x (\cos \theta \cos \psi) - W_y (\cos \theta \sin \psi)$$

$$\bar{v} = v - W_x (\cos \psi \sin \theta \sin \phi - \sin \psi \cos \phi) \\ - W_y (\cos \psi \cos \phi + \sin \psi \sin \theta \sin \phi)$$

$$\bar{w} = w - W_x (\cos \psi \sin \theta \cos \phi + \sin \psi \sin \phi) \\ - W_y (\sin \psi \sin \theta \cos \phi - \cos \psi \sin \phi)$$

Vehicle Position

$$\begin{aligned}\dot{X}_e &= u(\cos \theta \cos \psi) \\ &+ v(\cos \psi \sin \phi \sin \theta - \sin \psi \cos \phi) \\ &+ w(\cos \psi \cos \phi \sin \theta + \sin \psi \sin \phi) \\ \dot{Y}_e &= u(\cos \theta \sin \psi) \\ &+ v(\sin \psi \sin \phi \sin \theta + \cos \psi \cos \phi) \\ &+ w(\sin \psi \cos \phi \sin \theta - \cos \psi \sin \phi) \\ \dot{Z}_e &= -u(\sin \theta) + v(\sin \phi \cos \theta) + w(\cos \theta \cos \phi)\end{aligned}$$

Additional Equations

$$V_t = (\bar{u}^2 + \bar{v}^2 + \bar{w}^2)^{\frac{1}{2}}$$

$$q = \frac{1}{2} \rho V_t^2$$

$$\alpha_k = \tan^{-1} \frac{\bar{w}}{\bar{u}}$$

$$h = -Z$$

$$B = \sin^{-1} \frac{\bar{v}}{V_t}$$

Constants

$$m, I_x, I_y, I_z, I_{xz}, S, d, g, C_{L_\Delta}, C_{L_\beta}, C_{L_p}, C_{m_\alpha}, C_{m_q}, C_{n_\beta}, C_{n_\Delta}, C_{n_r}, \\ C_{y_\beta}, C_{y_\Delta}$$

Vehicle Inputs

$$\psi, \theta, \phi, u, v, w, p, q, r, X_e, Y_e, Z_e$$

Functions of h

ρ, W_x, W_y

Functions of α_k

C_x, C_z

Control Inputs

α_t, Δ

APPENDIX B

AERODYNAMIC DATA

The aerodynamics used in the simulation reflect the geometric change in the configuration caused by longitudinal and lateral control inputs. Aerodynamic force coefficients C_x and C_z are presented in figure 28.

The rest of the aerodynamic coefficients are expressed in derivative form as follows:

$$C_{l_{\Delta}} - .875 \text{ in/in}$$

$$C_{l_{\beta}} - .0017/\text{deg}$$

$$C_{l_p} - 1.306/\text{rad}$$

$$C_{m_{\alpha}} - .008/\text{deg}$$

$$C_{m_q} - .1146/\text{rad}$$

$$C_{n_{\beta}} .00075/\text{deg}$$

$$C_{n_{\Delta}} - .073 \text{ in/in}$$

$$C_{n_r} - .0229/\text{rad}$$

$$C_{Y_{\beta}} - .03/\text{deg}$$

$$C_{Y_{\Delta}} - 12 \text{ in/in}$$

Except for the control terms, all the coefficients are stability deviations. Therefore, a coordinate transformation from the stability to body axis must be performed so that they can be used in the equations-of-motion.

TABLE I. - PHYSICAL CHARACTERISTICS
OF GEMINI SPACECRAFT SIMULATED

Mass (m)	139.82	slugs
Roll inertia (I_x)	4870	slug-ft ²
Pitch inertia (I_y)	5493	slug-ft ²
Yaw inertia (I_z)	2427	slug-ft ²
Product of inertia in the X_b, Z_b plane (I_{xz})	-910	slug-ft ²
Keel length (d)	30.58	ft
Reference area (S)	536.2	ft ²
Forward shroud length (l_2/l_R)	.695	in/in
Aft shroud length (l_1/l_R) (steady state of glide)	.56	in/in

TABLE II. - TEST CASES

Category (A) Radar accuracies							
Case	Desired runway	Initial position			Wind profile	Wind error	Radar error
		X _e	Y _e	Z _e			
A-1	130°	25K	25K	40K	1-S	10%	1°
A-2	130°	50K	50K	40K	1-S	10%	1°
A-3	130°	-50K	-50K	40K	1-S	10%	2°
A-4	130°	-50K	100K	40K	1-S	10%	2°
A-5	130°	-50K	100K	40K	1-S	10%	0°
Category (B) Wind effects							
Case	Desired runway	Initial position			Wind profile	Wind error	Radar error
		X _e	Y _e	Z _e			
B-1	40°	50K	50K	40K	4-S	10%	1°
B-2	40°	50K	50K	40K	4-S gusts	10%	1°
B-3	40°	50K	50K	40K	4-S	20%	1°
B-4	40°	50K	50K	40K	4-S gusts	20%	1°
B-5	40°	50K	50K	40K	2-S	30%	1°
B-6	40°	50K	50K	40K	2-S gusts	30%	1°
B-7	350°	-100K	50K	40K	1-W	0	1°
B-8	350°	-100K	50K	40K	1-W	10%	1°
B-9	350°	-100K	100K	40K	1-W	20%	1°
B-10	350°	-100K	0	40K	1-W	30%	1°
B-11	350°	-100K	100K	40K	1-W gusts	0	1°
B-12	350°	-100K	100K	40K	1-W gusts	10%	1°
Category (C) Initial position							
Case	Desired runway	Initial position			Wind profile	Wind error	Radar error
		X _e	Y _e	Z _e			
C-1	130°	0	82K	40K	1-S	10%	1°
C-2	130°	0	109K	40K	1-S	10%	1°
C-3	130°	0	119K	40K	1-S	10%	1°
C-4	130°	122K	0	40K	1-S	10%	1°
C-5	130°	128.5K	0	40K	1-S	10%	1°
C-6	350°	128.5K	0	40K	1-W	10%	1°
C-7	310°	-135K	0	40K	3-S	10%	1°
C-8	310°	-135K	0	40K	3-S	10%	1°
C-9	310°	-139K	0	40K	3-S	10%	1°
Category (D) Cross wind and wind gusts							
Case	Desired runway	Initial position			Wind profile	Wind error	Radar error
		X _e	Y _e	Z _e			
D-1	350°	-50K	-50K	40K	3-S gusts	10%	1°
D-2	350°	25K	25K	20K	3-S gusts	10%	1°

TABLE II. - TEST CASES - Continued

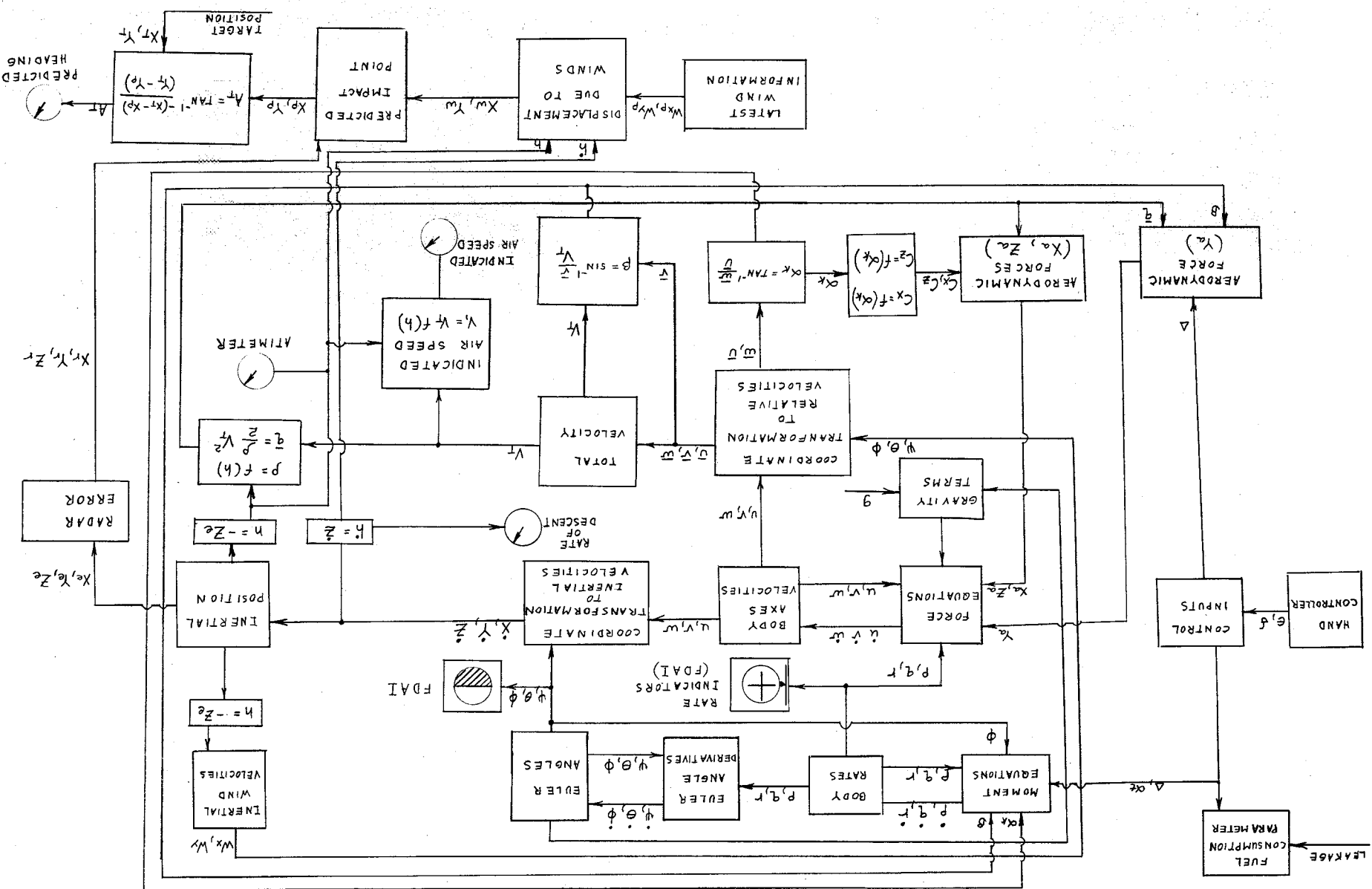
Category (E) System failures and alternate procedures (Note: All wind errors are 10%; all radar errors are 1°)						
Case	Desired runway	Initial position			Wind profile	Type of approach
		X _e	Y _e	Z _e		
E-1	130°	25K	25K	40K	1-S	No heading information. All turns relative.
E-2	130°	25K	25K	40K	1-S	No gyro approach. Start and stop all turns.
E-3	130°	25K	25K	40K	1-S	Orbit center of field. Intersect glide slope at 4K
E-4	130°	25K	25K	40K	1-S	Orbit center of field. Intersect glide slope at 3K
E-5	130°	25K	25K	40K	1-S	Orbit center of field. Intersect glide slope at 2K
E-6	40° to 130°	25K	25K	20K	4-S to 1-S	Change from measured wind at 8K
E-7	40° to 130°	25K	25K	20K	4-S to 1-S	Change from measured wind at 4K
E-8	40°	25K	25K	20K	4-S to 1-S	Change from measured wind at 3K
E-9	40°	25K	25K	20K	4-S to 1-S	Change wind at 3K. Use old glide slope
E-10	40°	25K	25K	20K	4-S	Orbit downwind end of runway. Intersect glide slope at low altitude.
E-11	40°	25K	25K	20K	4-S	Orbit downwind end of runway. Intersect glide slope at low altitude.
E-12	40°	25K	25K	20K	4-S	Orbit downwind end of runway. Intersect glide slope at low altitude.
E-13	40°	0	0	15K	4-S	Establish same holding pattern regardless of wind.
E-14	40°	0	0	15K	4-S	Establish same holding pattern regardless of wind.
E-15	40°	50K	50K	40K	4-S	Control system with rate command in roll.
E-16	40°	50K	50K	40K	4-S	Same as above using position command
E-17	40°	50K	50K	40K	4-S	All maneuvers done with half standard rate turns
E-18	40°	50K	50K	40K	4-S	All maneuvers done with quarter standard rate turns.

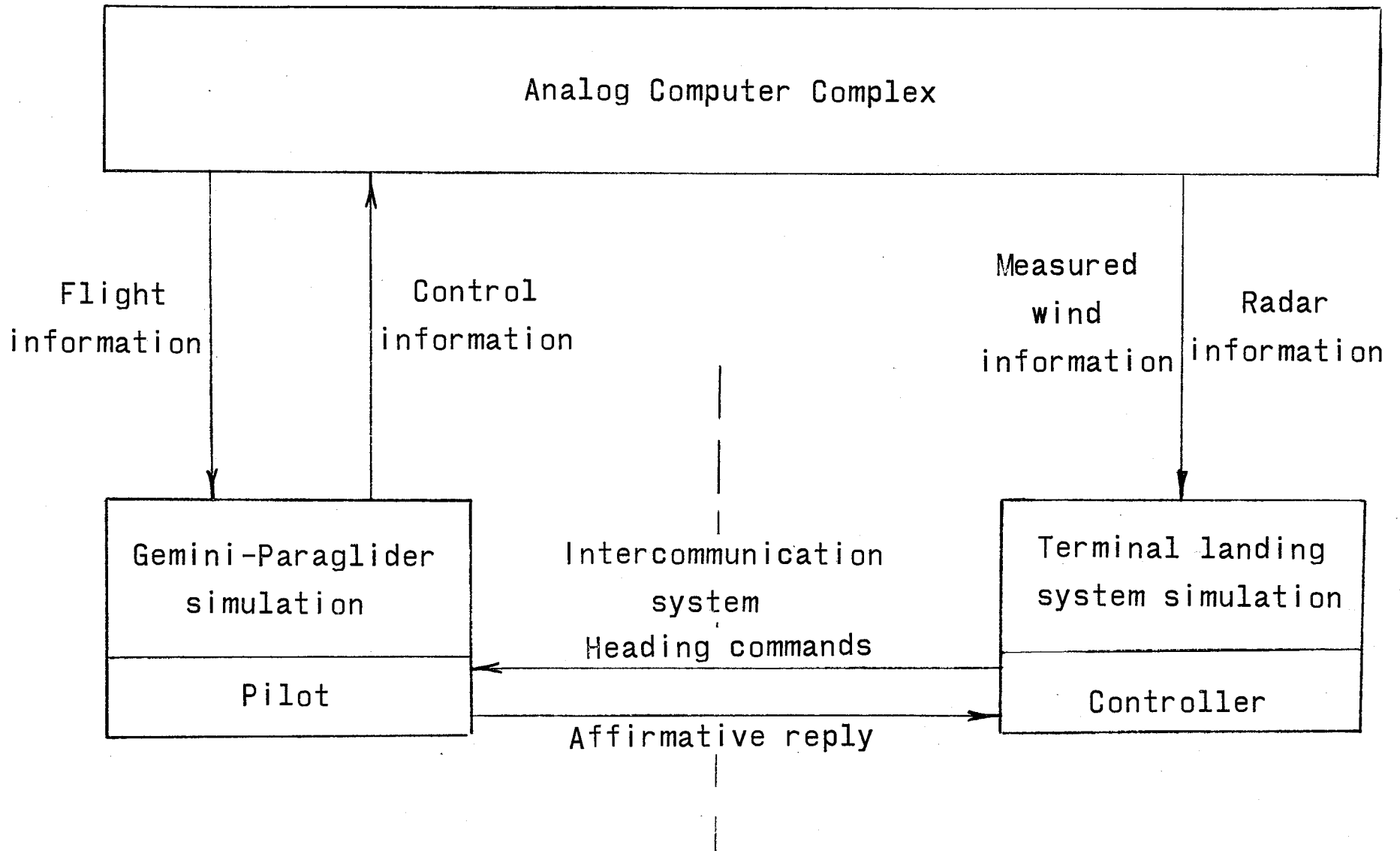
TABLE II. - TEST CASES - Concluded

Category (F) Automatic direction finding (ADF)							
(Note: There are no measured winds)							
Case	Desired runway	Initial position			Wind profile	Radar error	ADF location
		X _e	Y _e	Z _e			
F-1	130°	50K	50K	40K	S-1	1°	0
F-2	130°	50K	50K	40K	S-1	1°	1 nm
F-3	130°	25K	25K	40K	W-1	1°	.5 nm
F-4	130°	25K	25K	40K	W-1	1°	.2 nm
F-5	130°	10K	10K	40K	S-1	1°	1 nm
F-6	130°	10K	10K	40K	W-1	1°	1 nm

Figure 1.- Block diagram of analog simulation.

(a) Computer math flow.





(b) Pilot-controller information flow.
Figure 1.- Concluded.

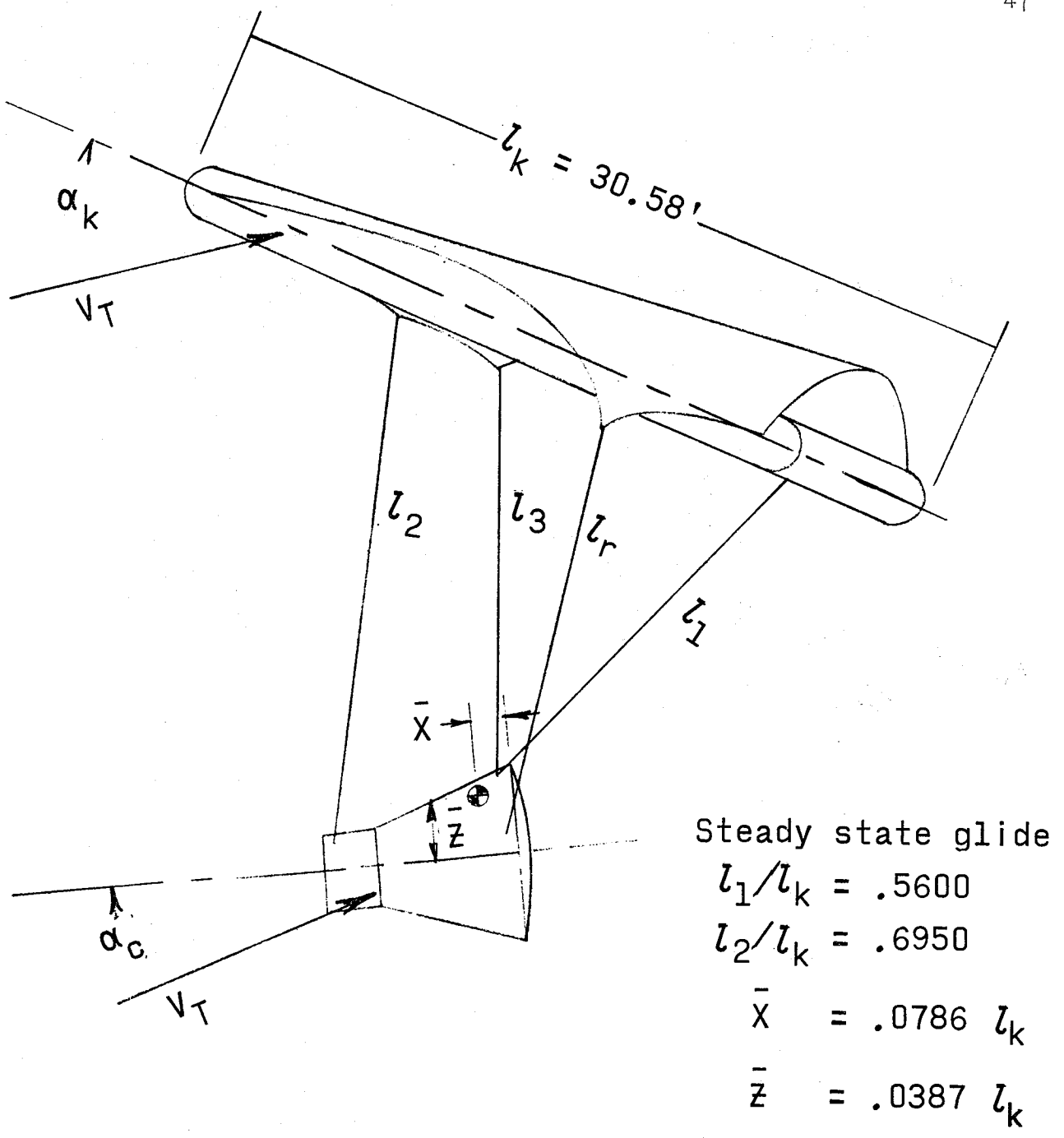


Figure 2.- General dimensions of simulated vehicle.

Note: X_b axis is parallel to wing keel.

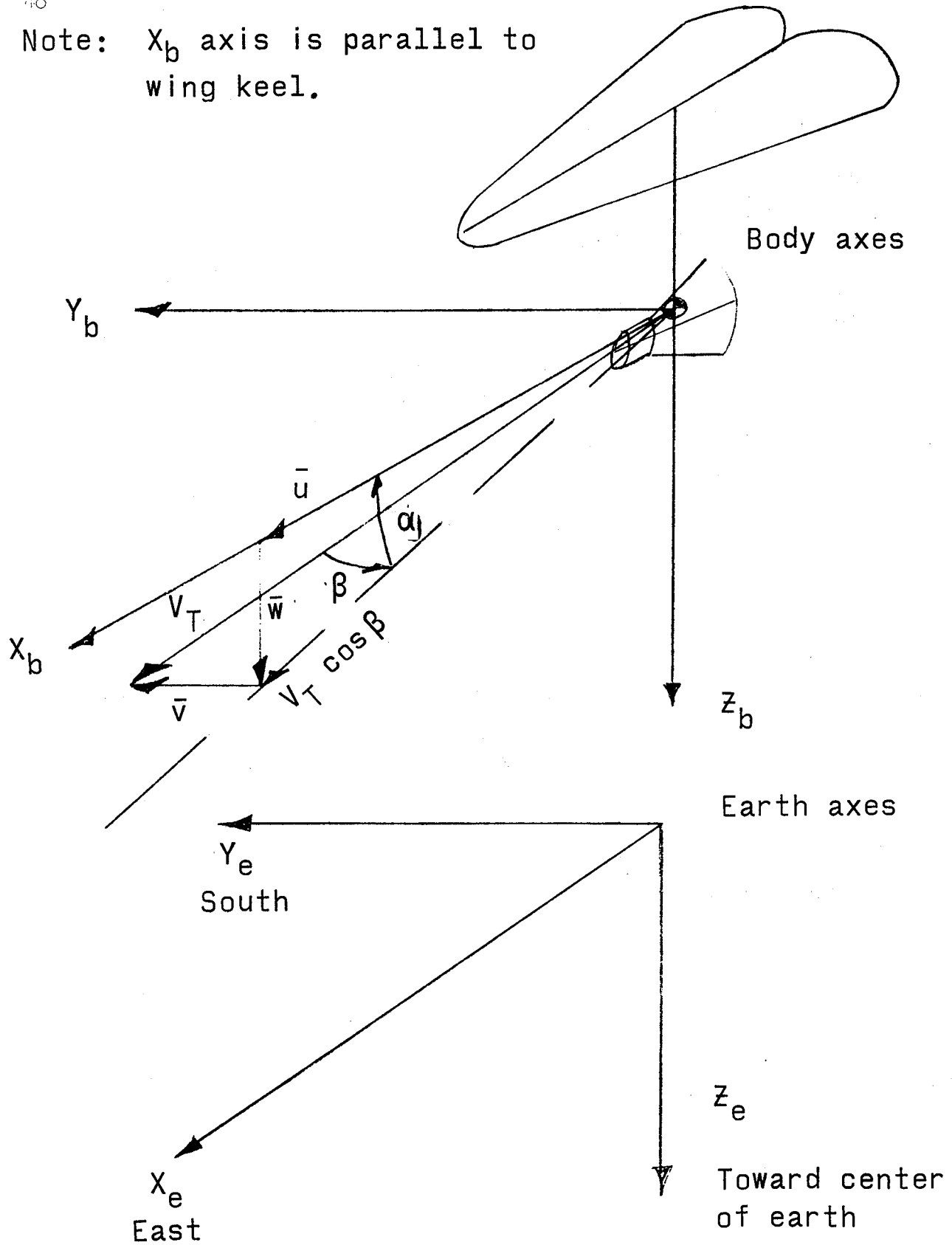


Figure 3.- Body and earth fixed axes systems.

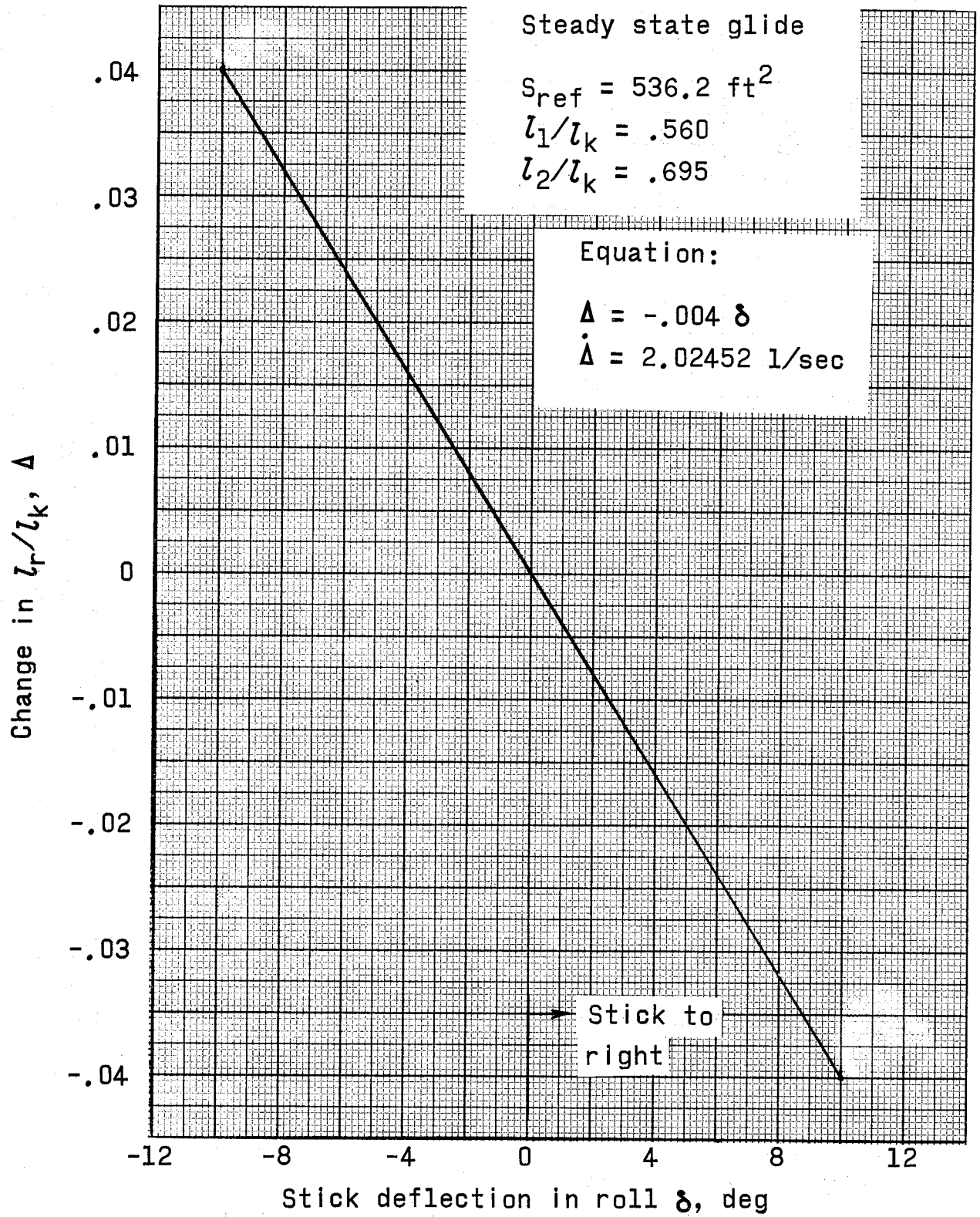
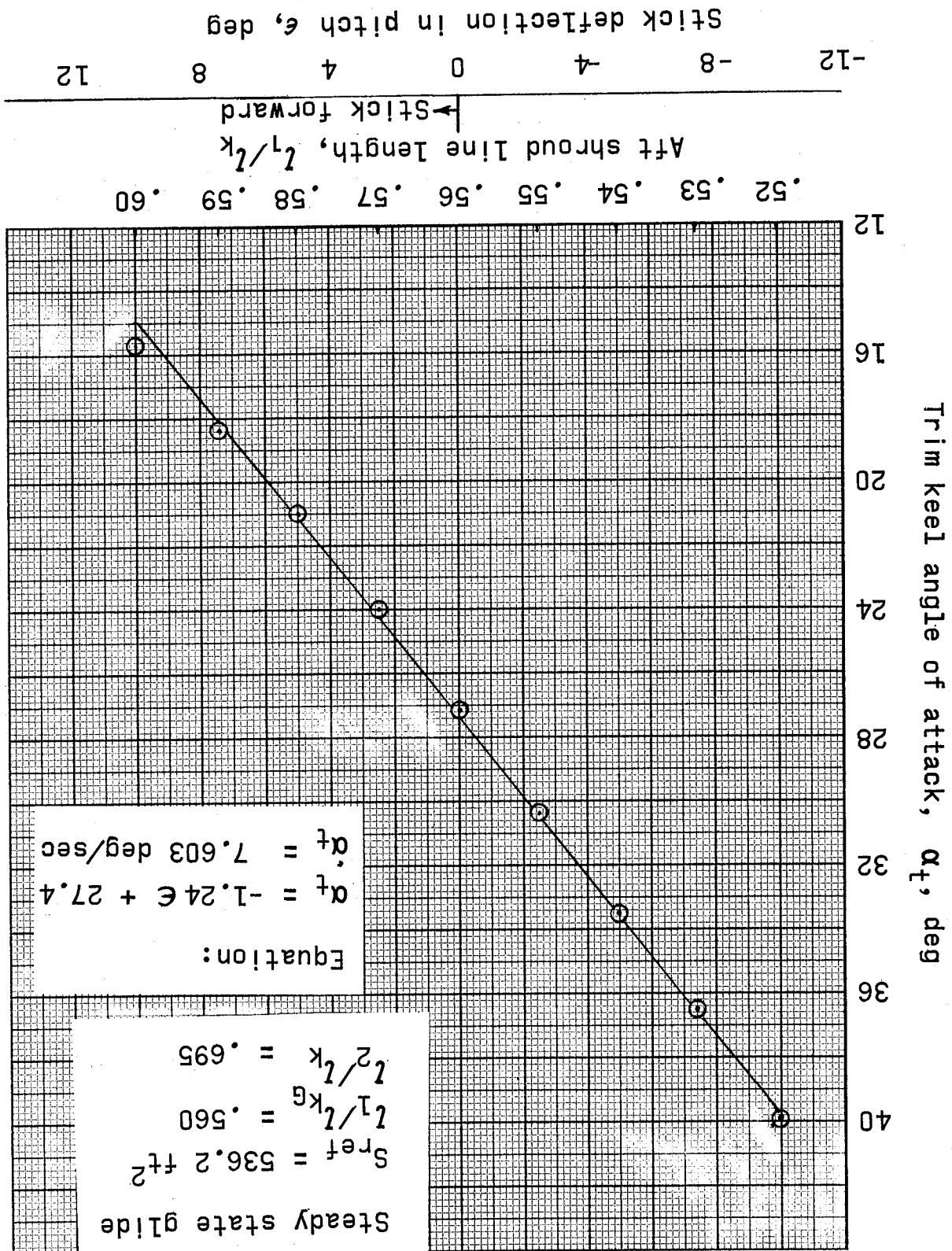


Figure 4.- Change in lateral shroud length (l_r) versus stick deflection in roll (δ).

Figure 5. - Change in trim angle of attack (α_t) versus stick deflection in pitch (ϵ).



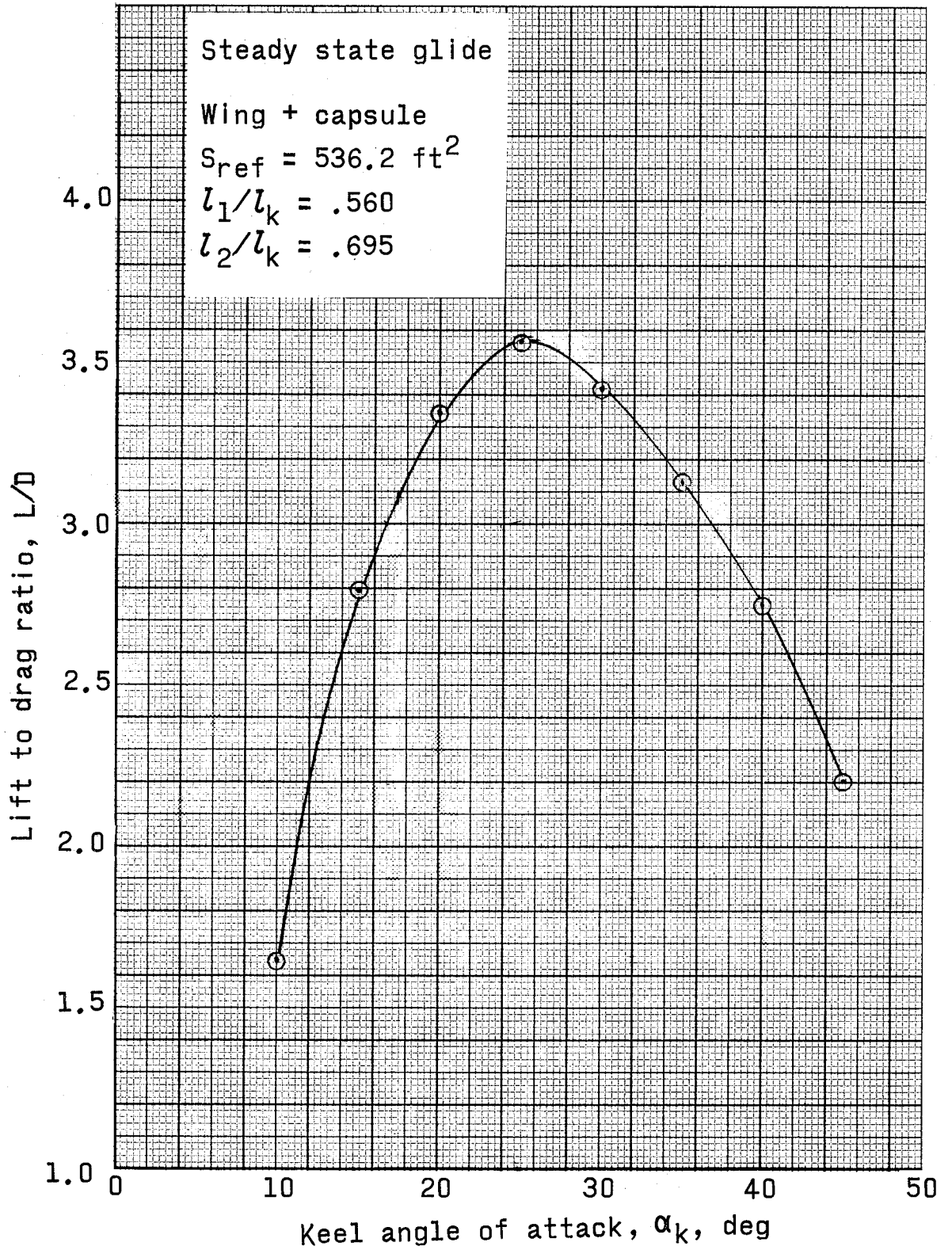


Figure 6.- Lift to drag ratio (L/D) versus keel angle of attack (α_k).

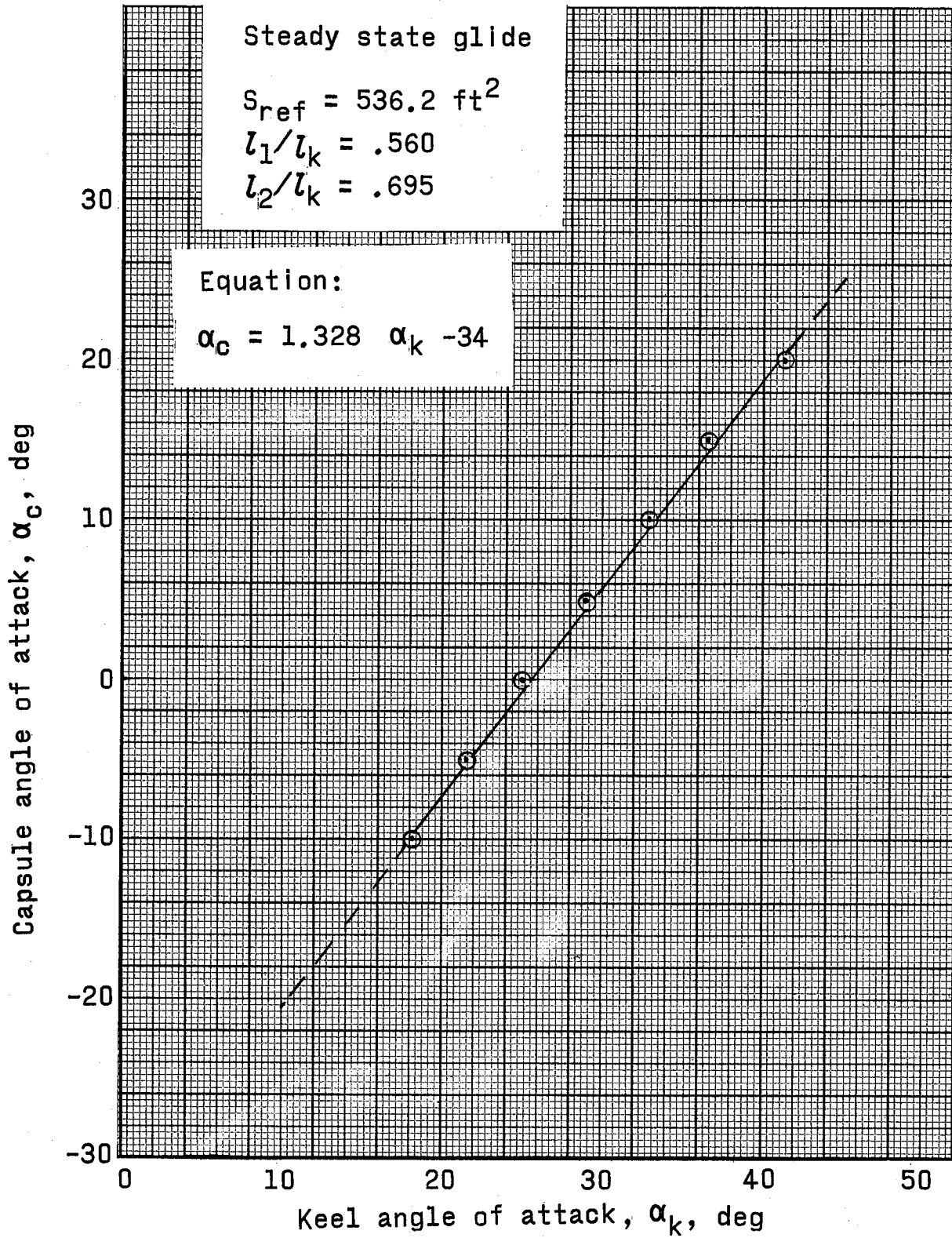


Figure 7.- Capsule angle of attack (α_c) versus keel angle of attack (α_k).

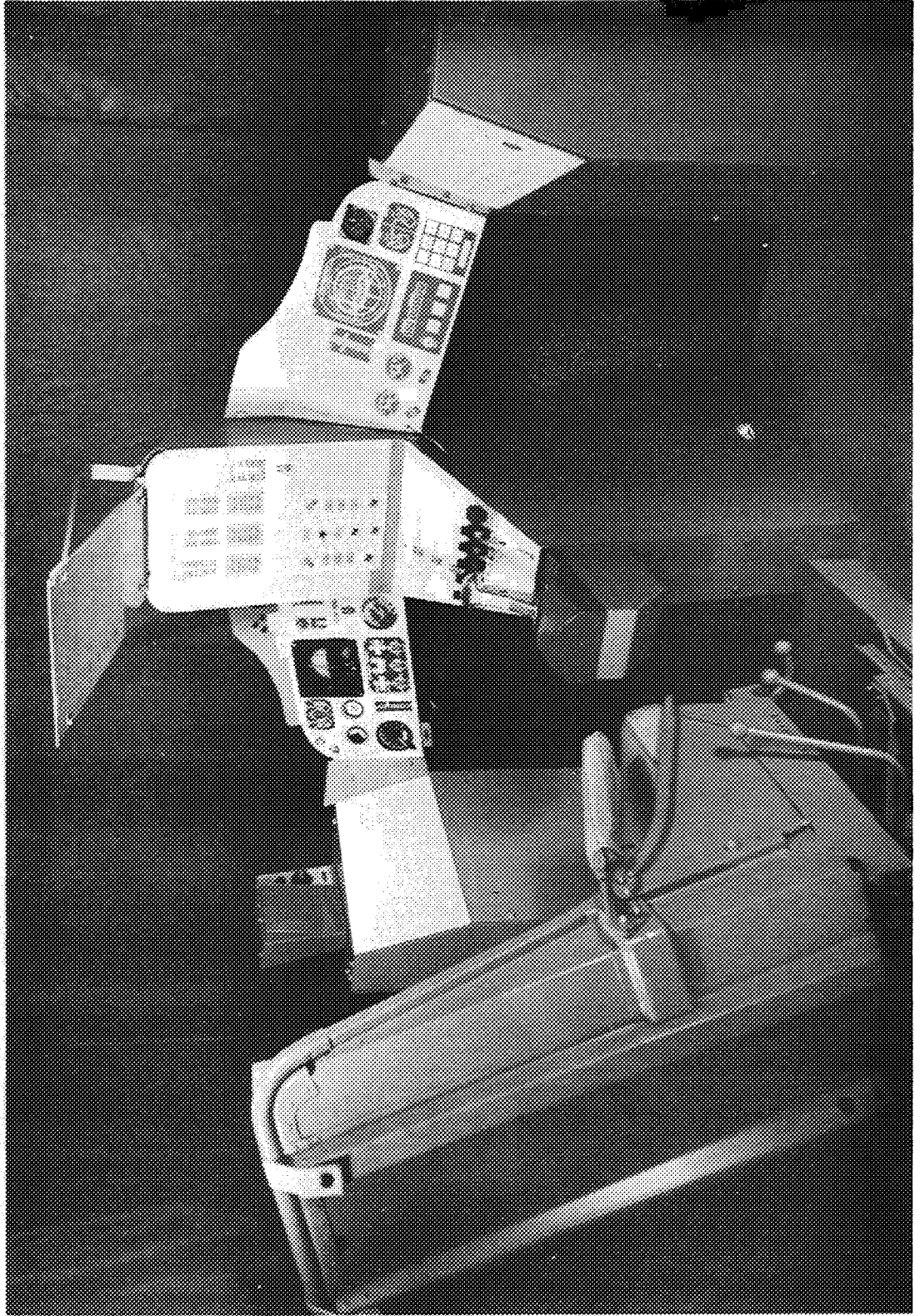
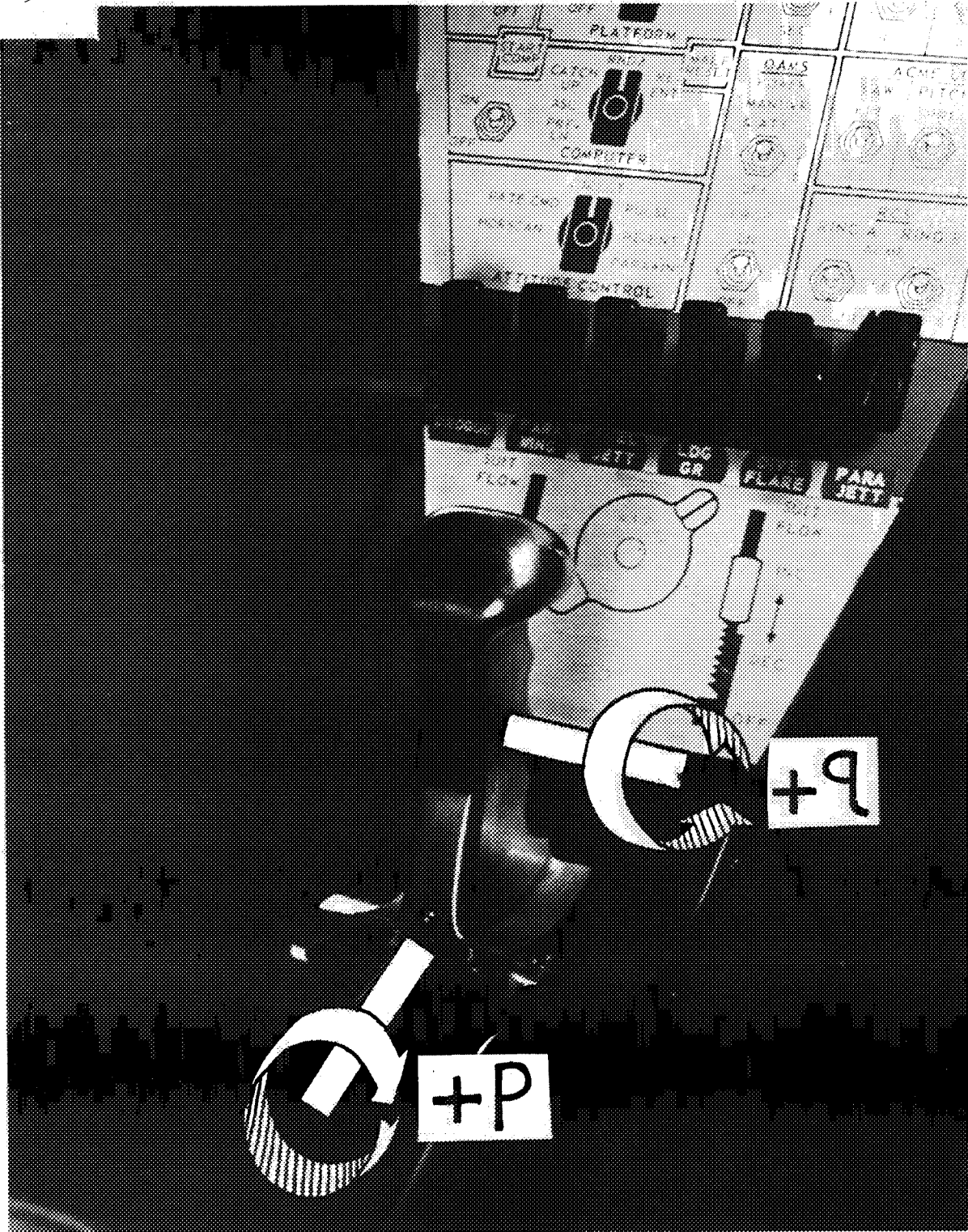
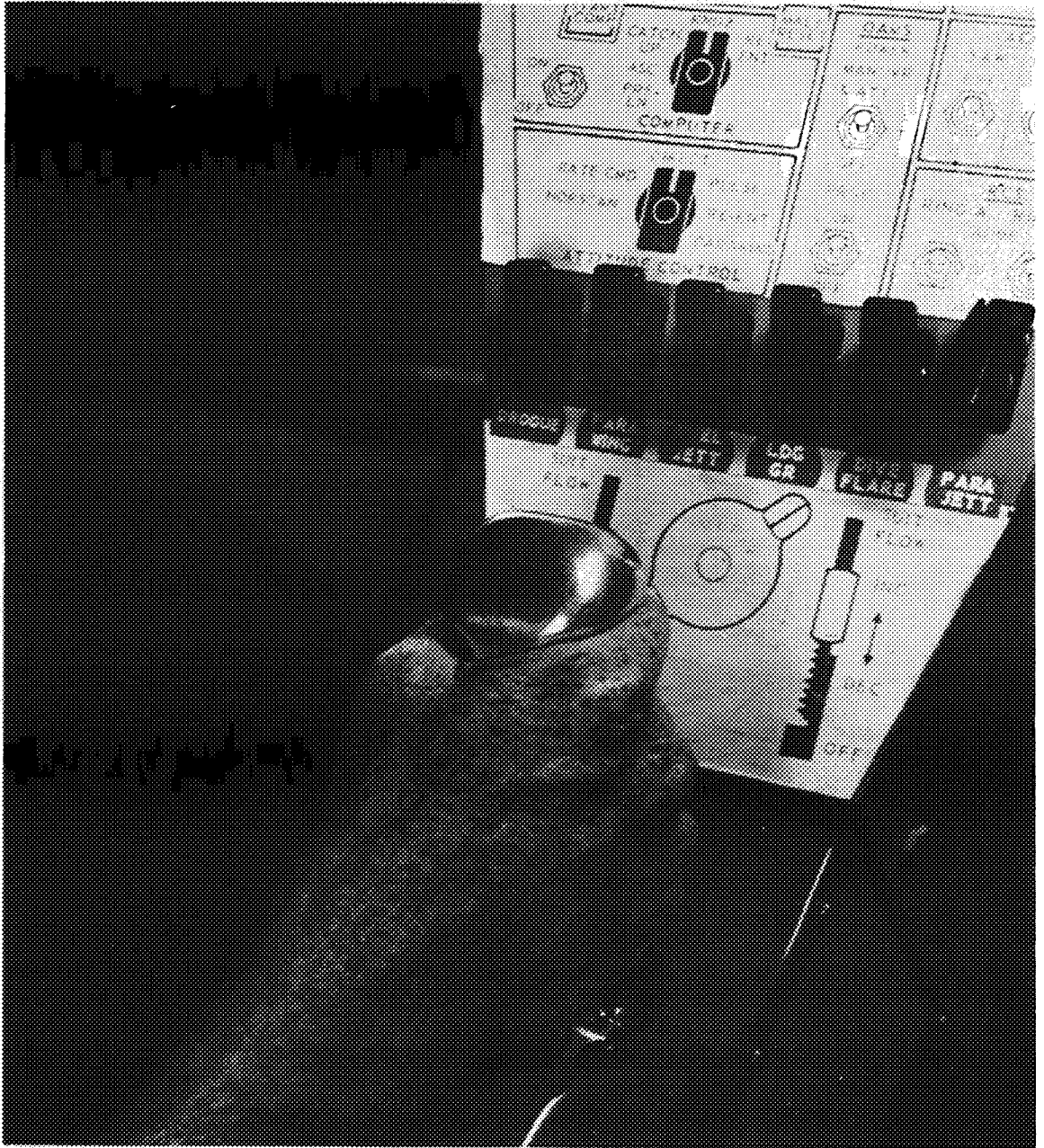


Figure 8. - Simulator cockpit.



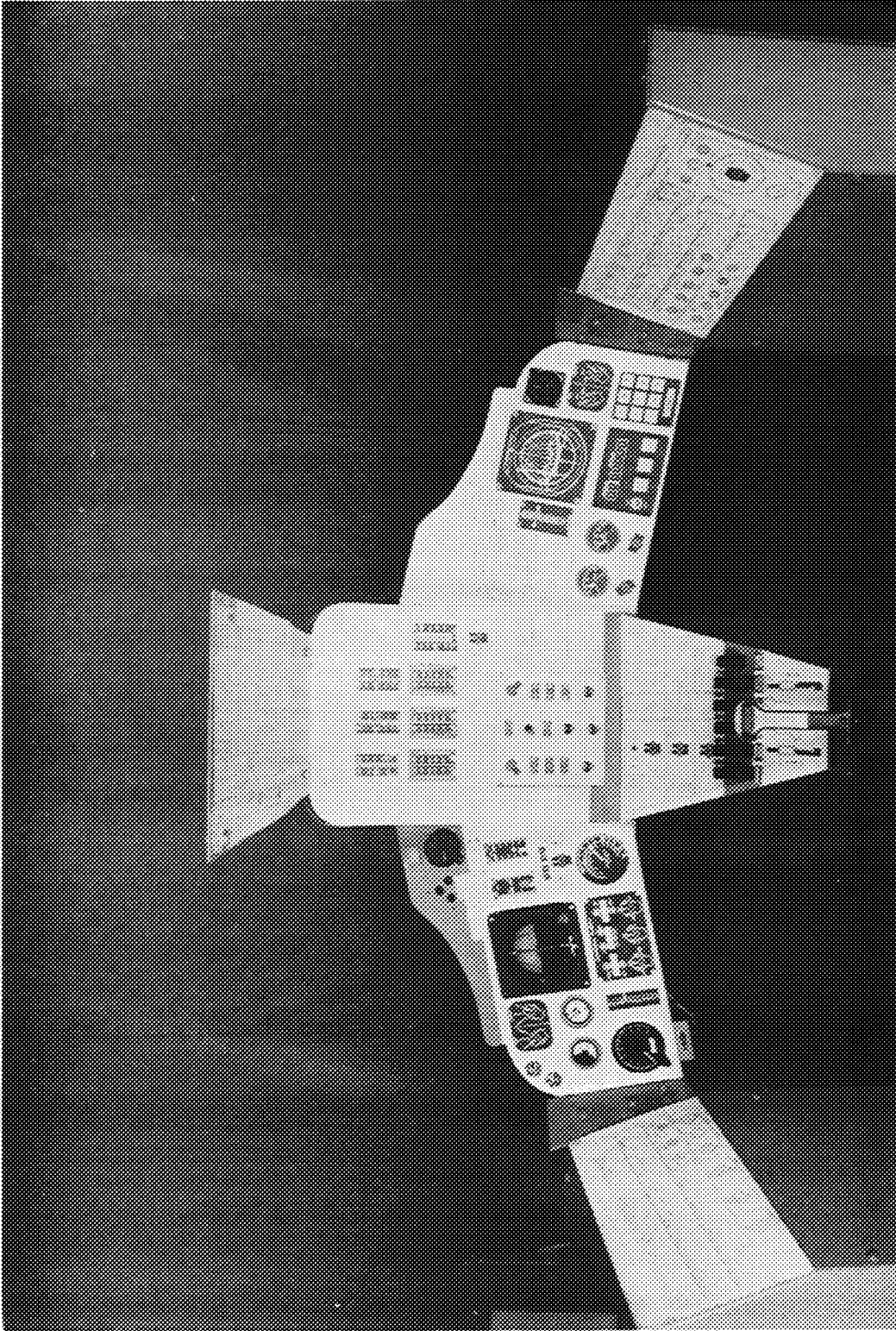
(a) Resultant motion.

Figure 9.- Hand controller.



(b) Pilot's hand position.

Figure 9.- Concluded.



(a) Complete console.
Figure 10.- Display panel.

(b) Command astronaut's console.

Figure 10 - Concluded

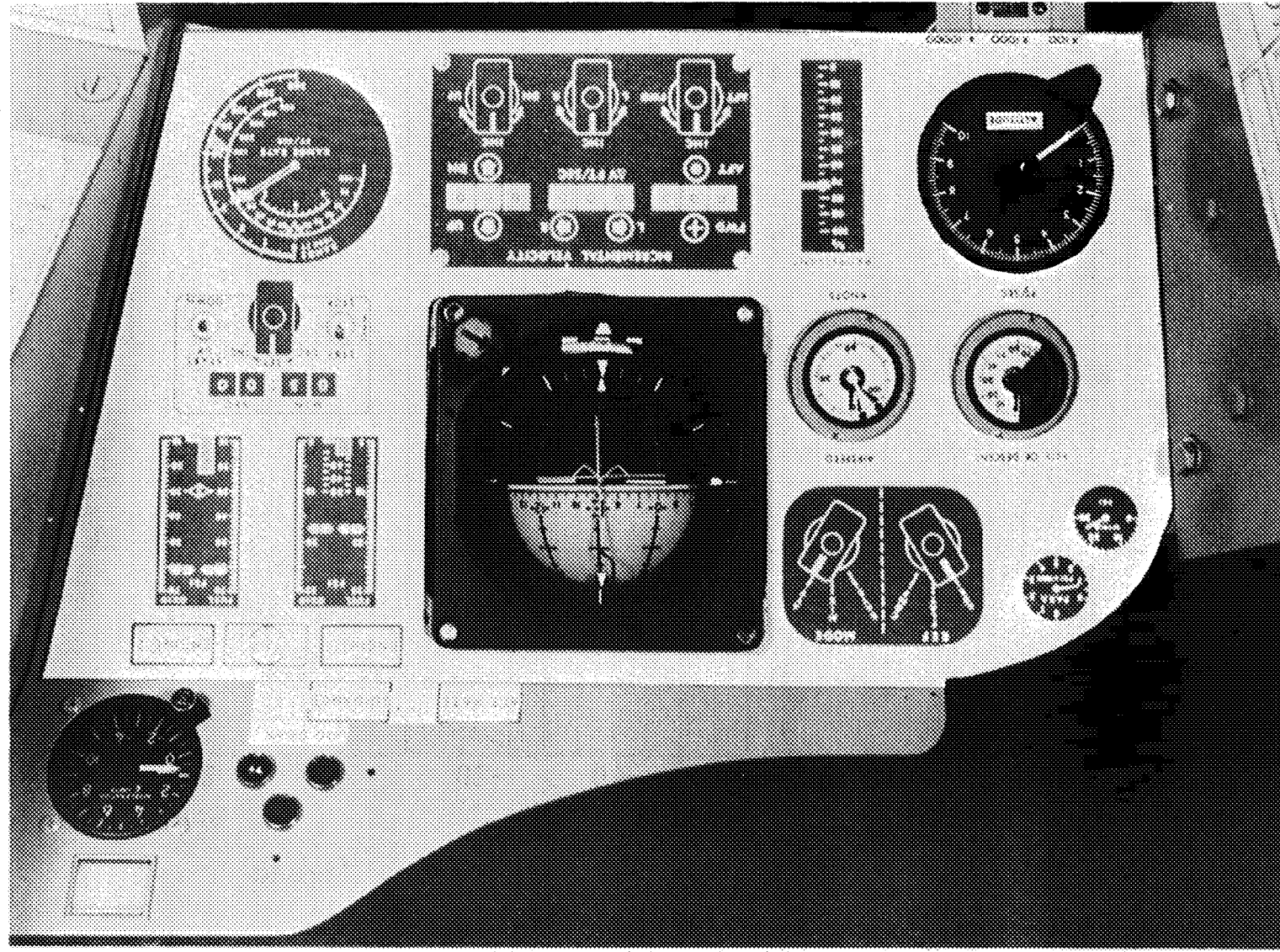
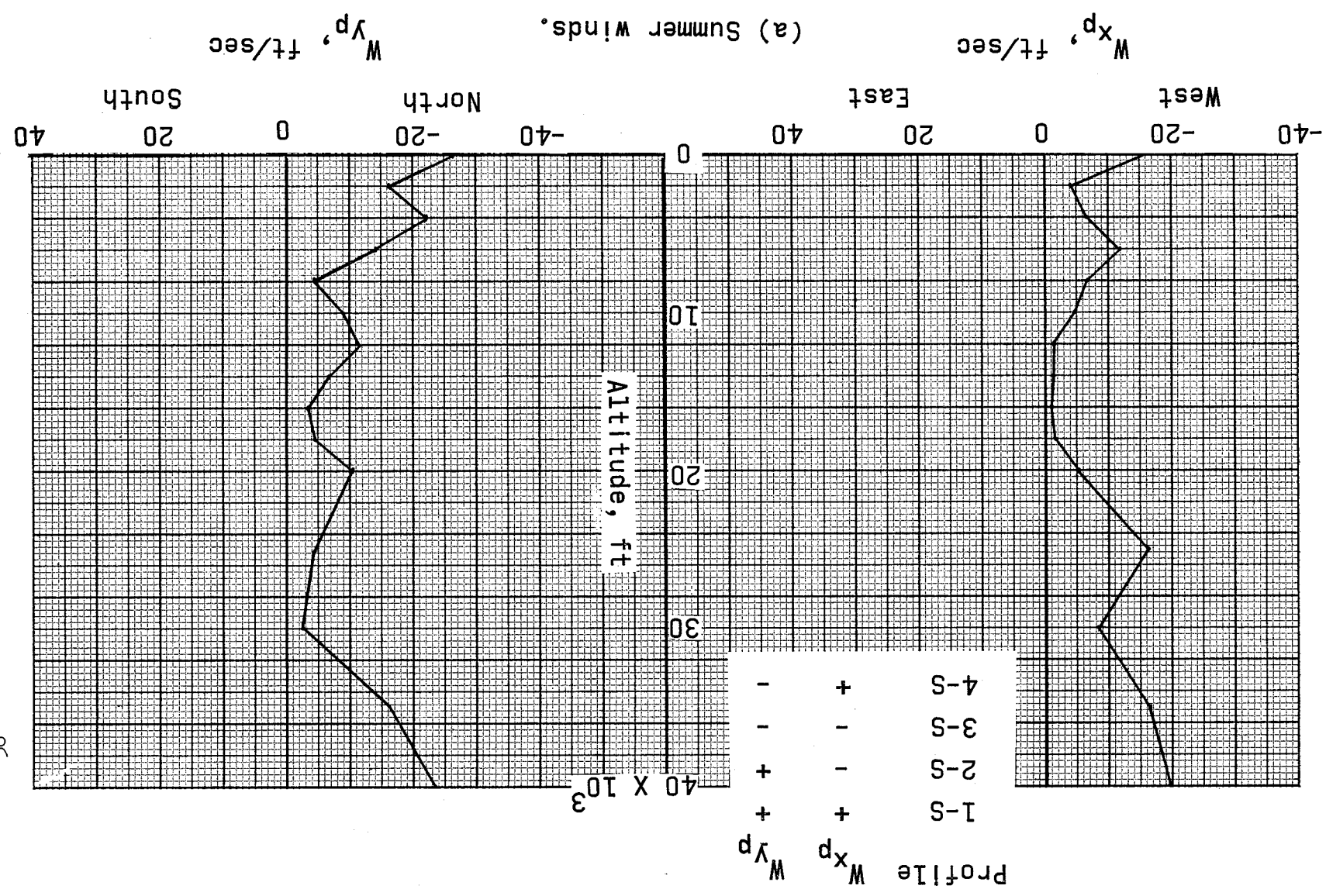
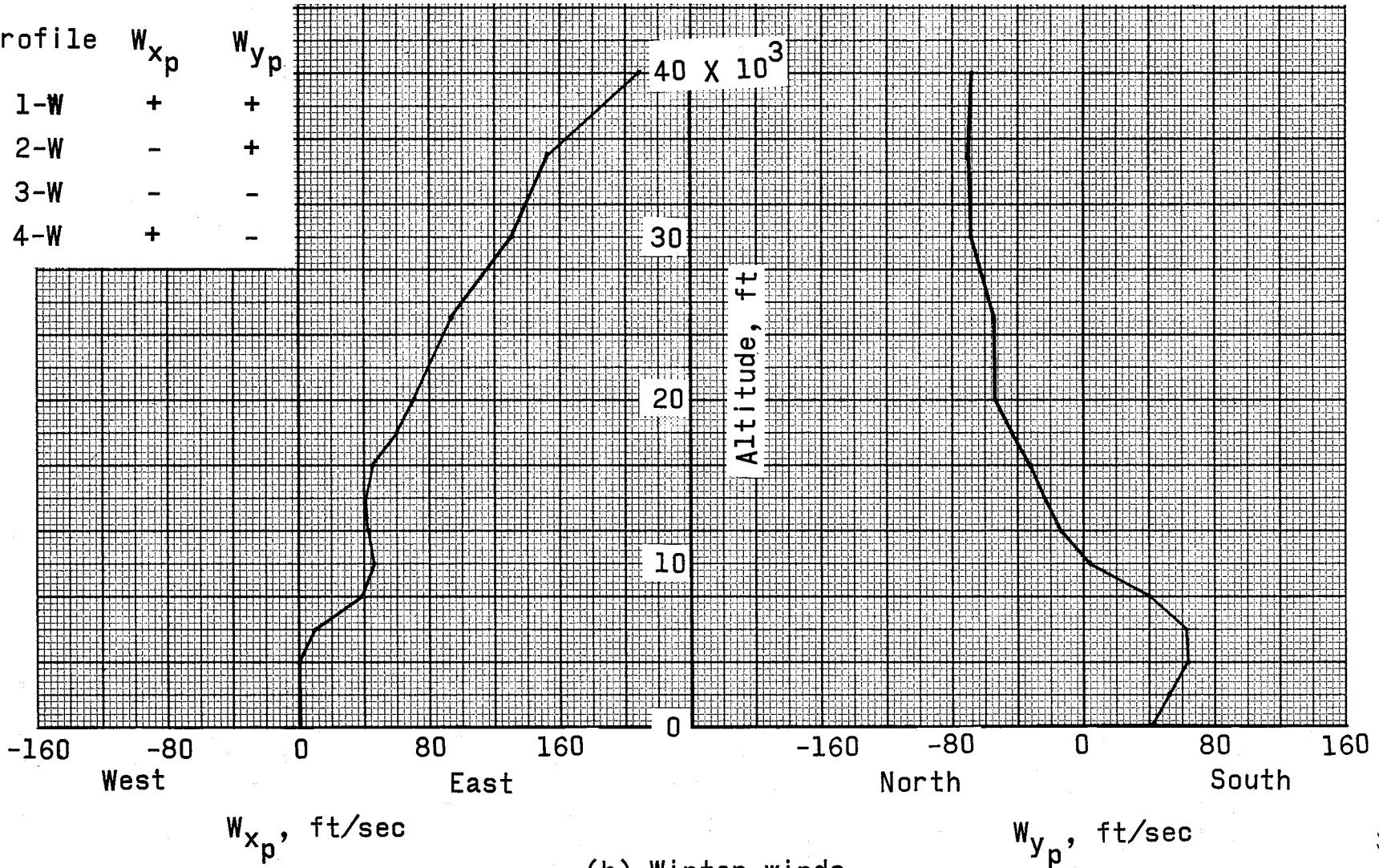


Figure 11. - Wind profiles used in the simulation.



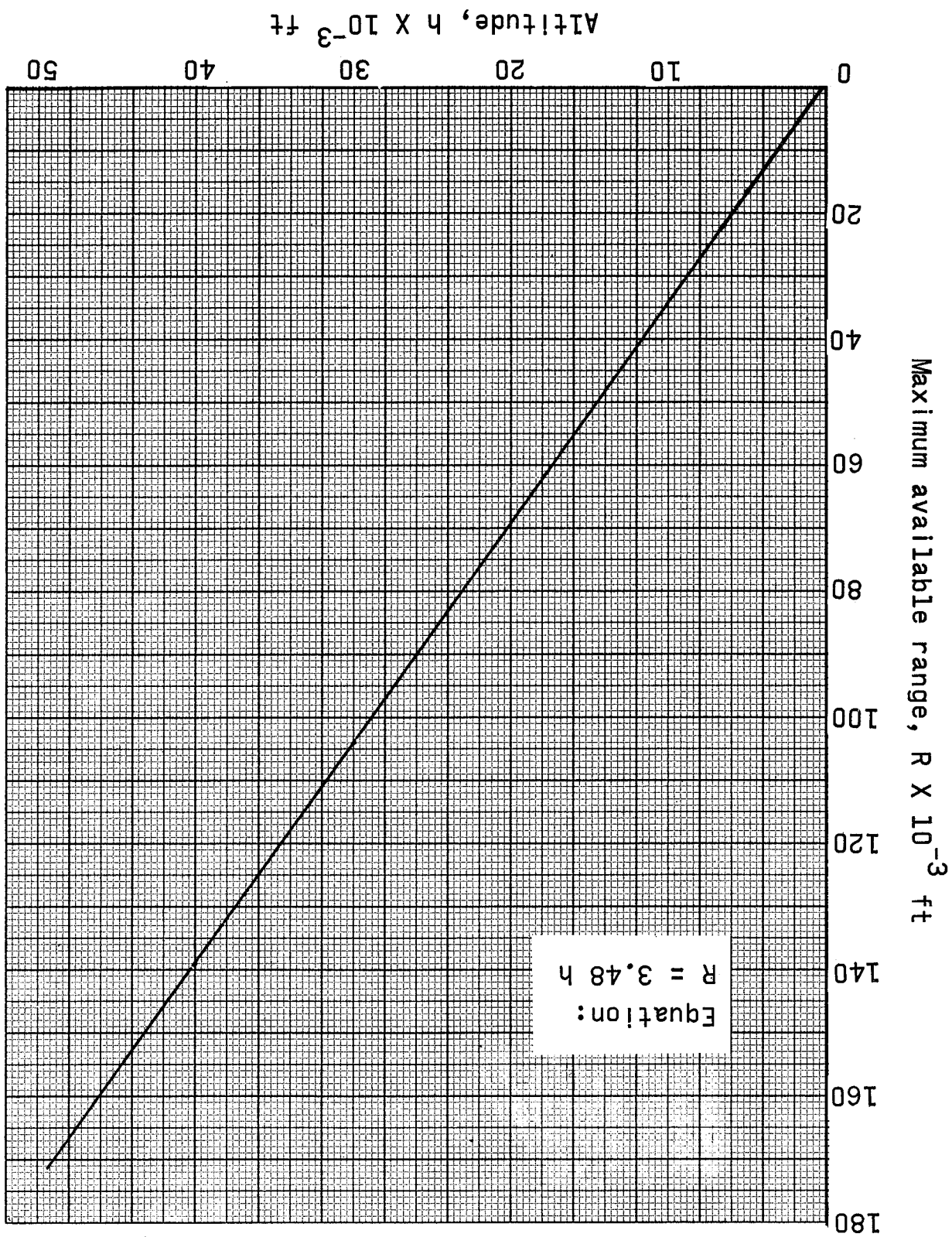
Profile	W_{xp}	W_{yp}
1-W	+	+
2-W	-	+
3-W	-	-
4-W	+	-



(b) Winter winds.

Figure 11.- Concluded.

Figure 12.- Maximum available range versus altitude.



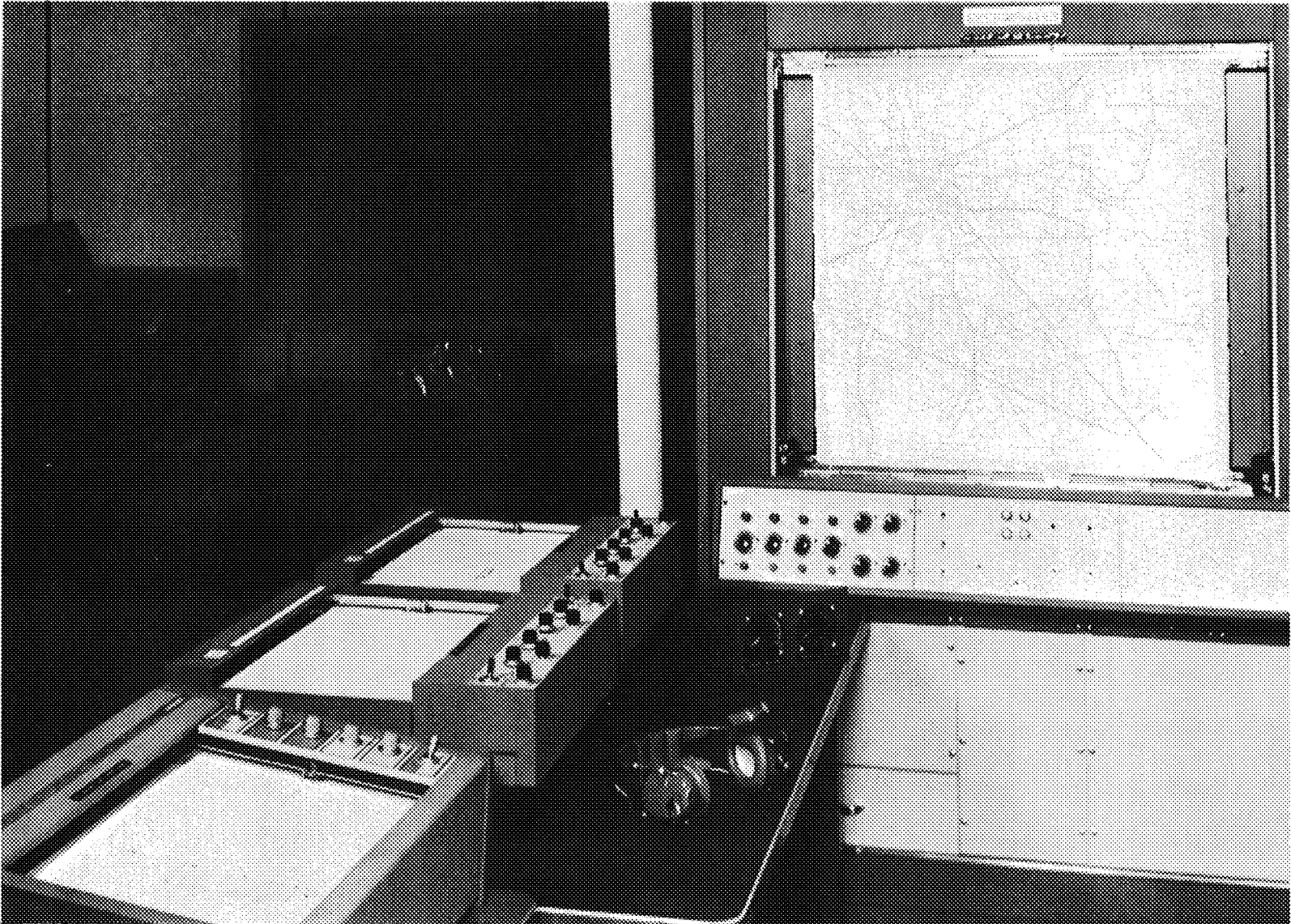


Figure 13.- Terminal landing system simulation.

Figure 14.- Preselcted target plus surrounding area (30 in. by 30 in. X-Y plotter).

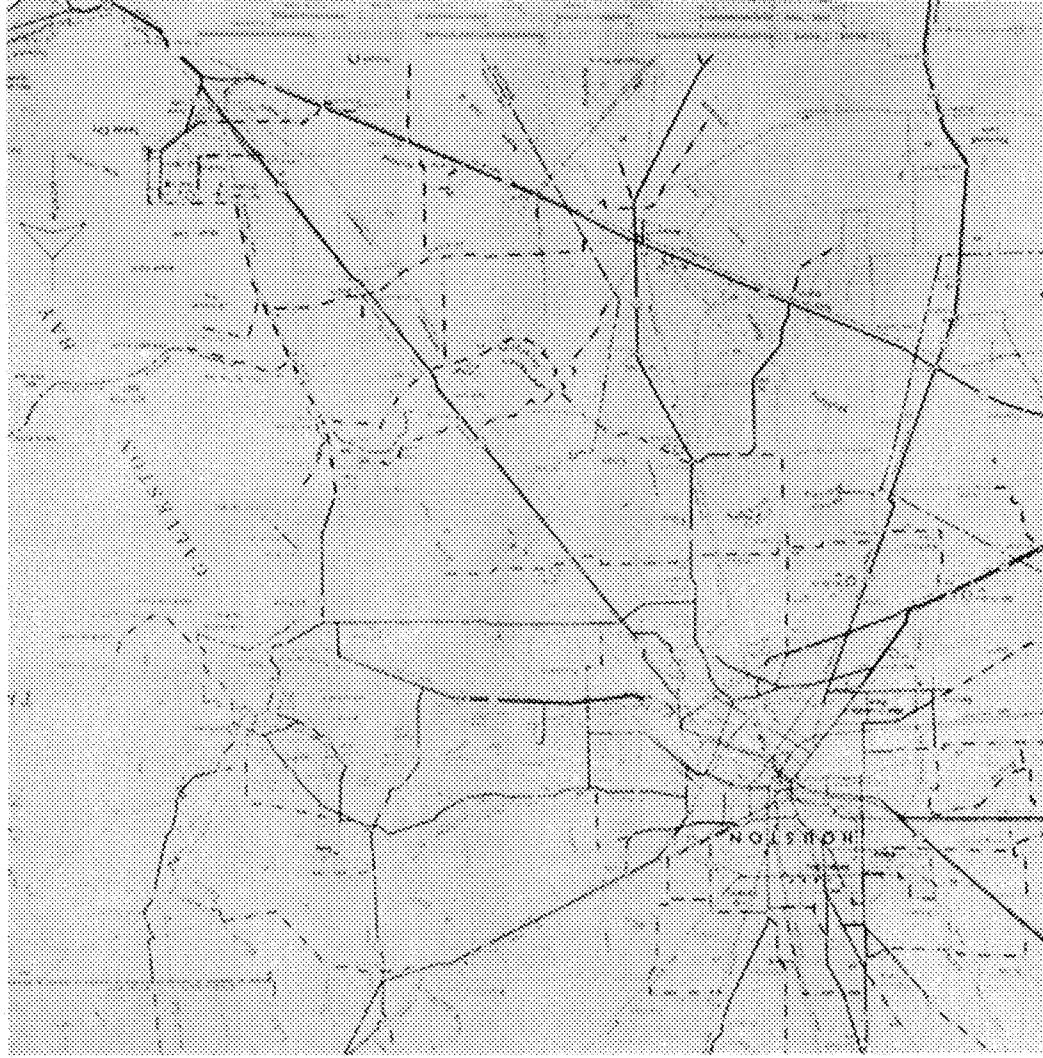
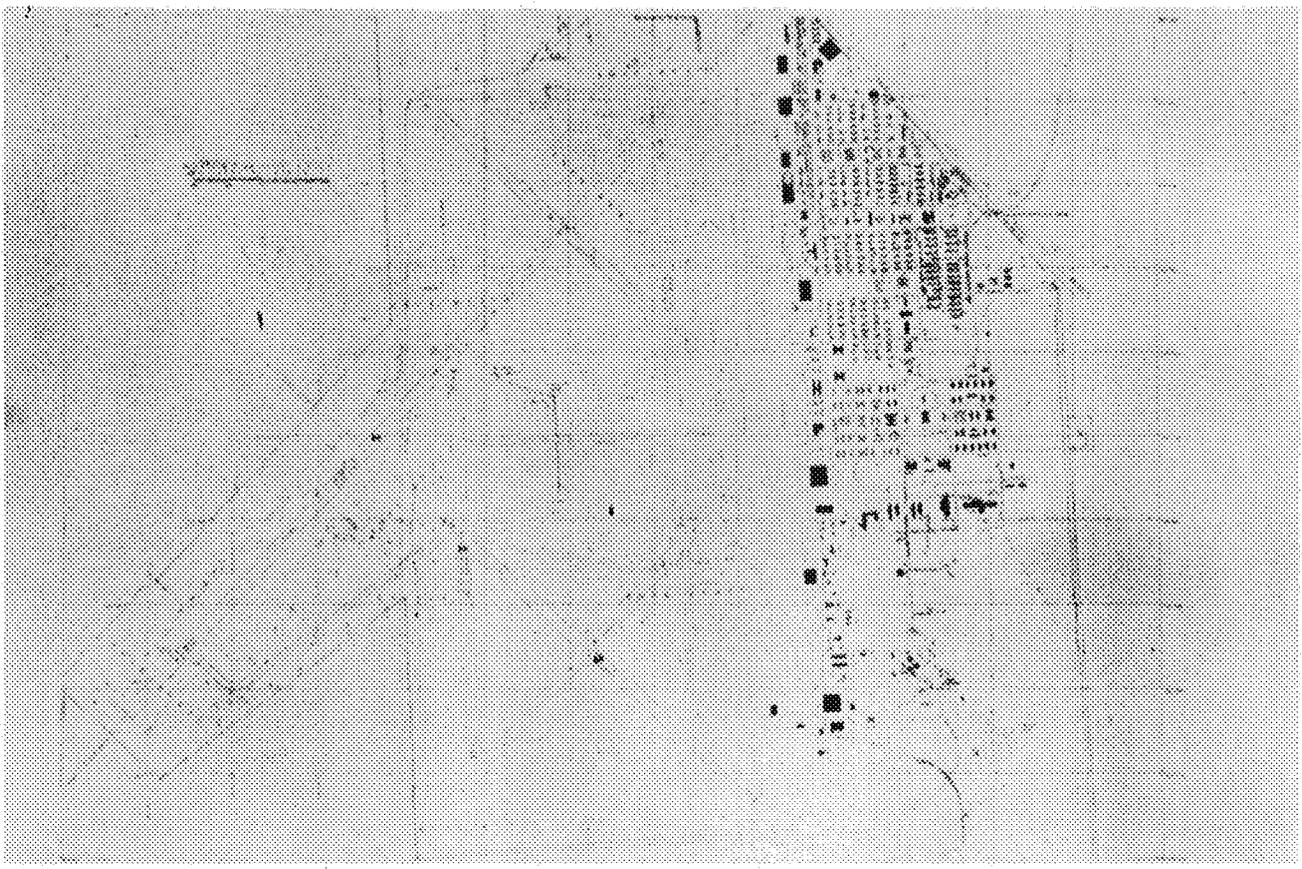


Figure 15.- ELLINGTON air force base (10 in. by 15 in. X-Y plotter).



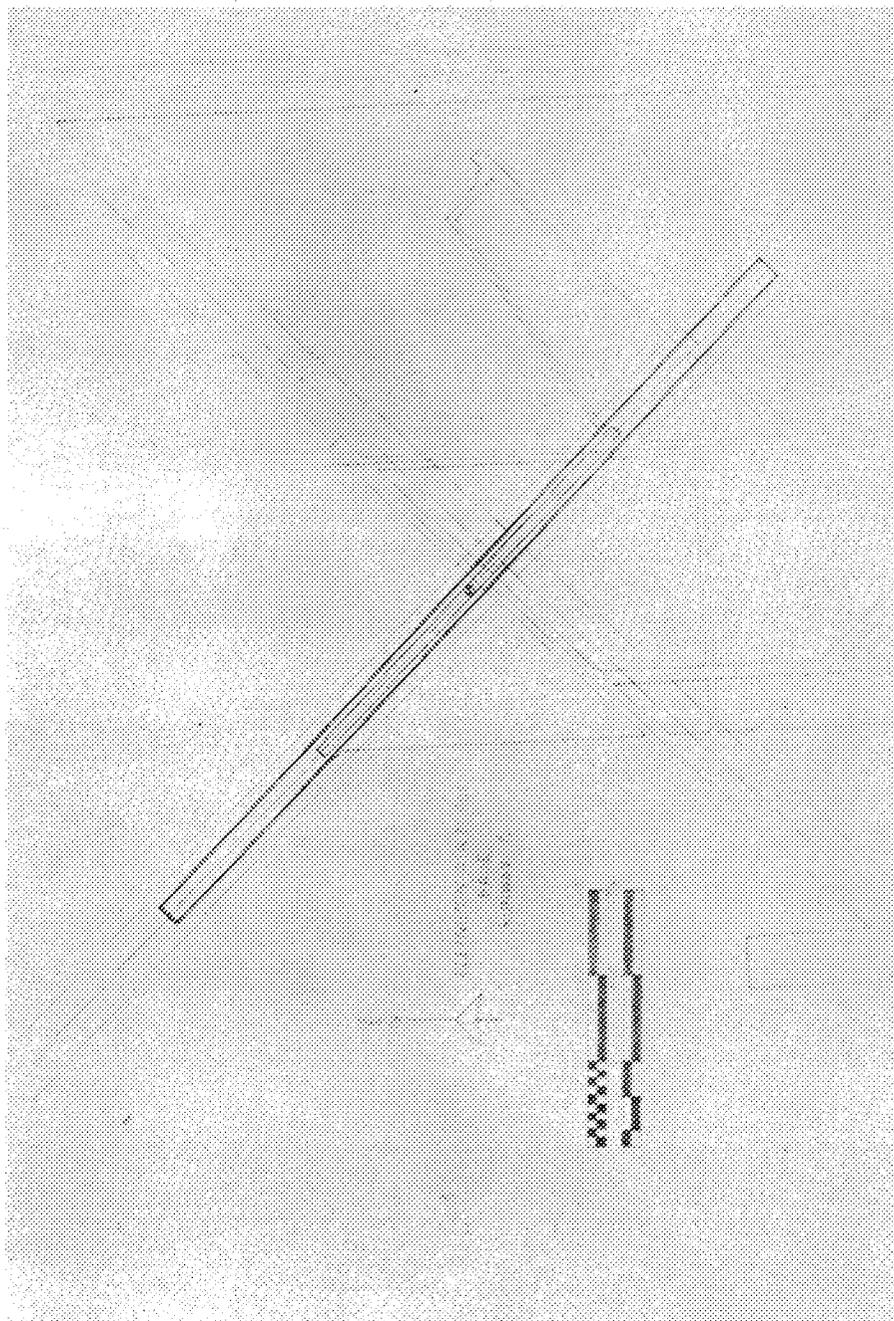
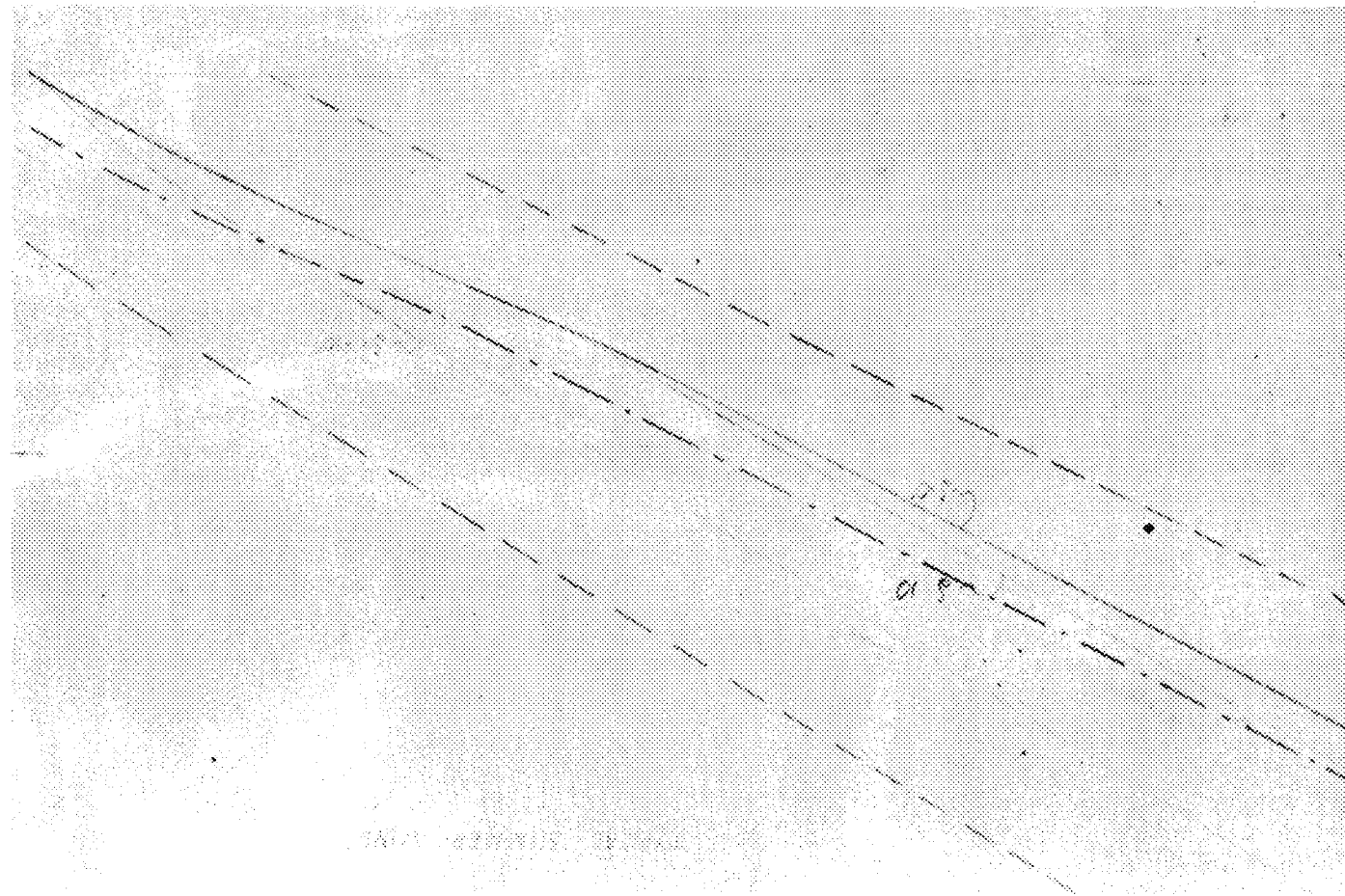
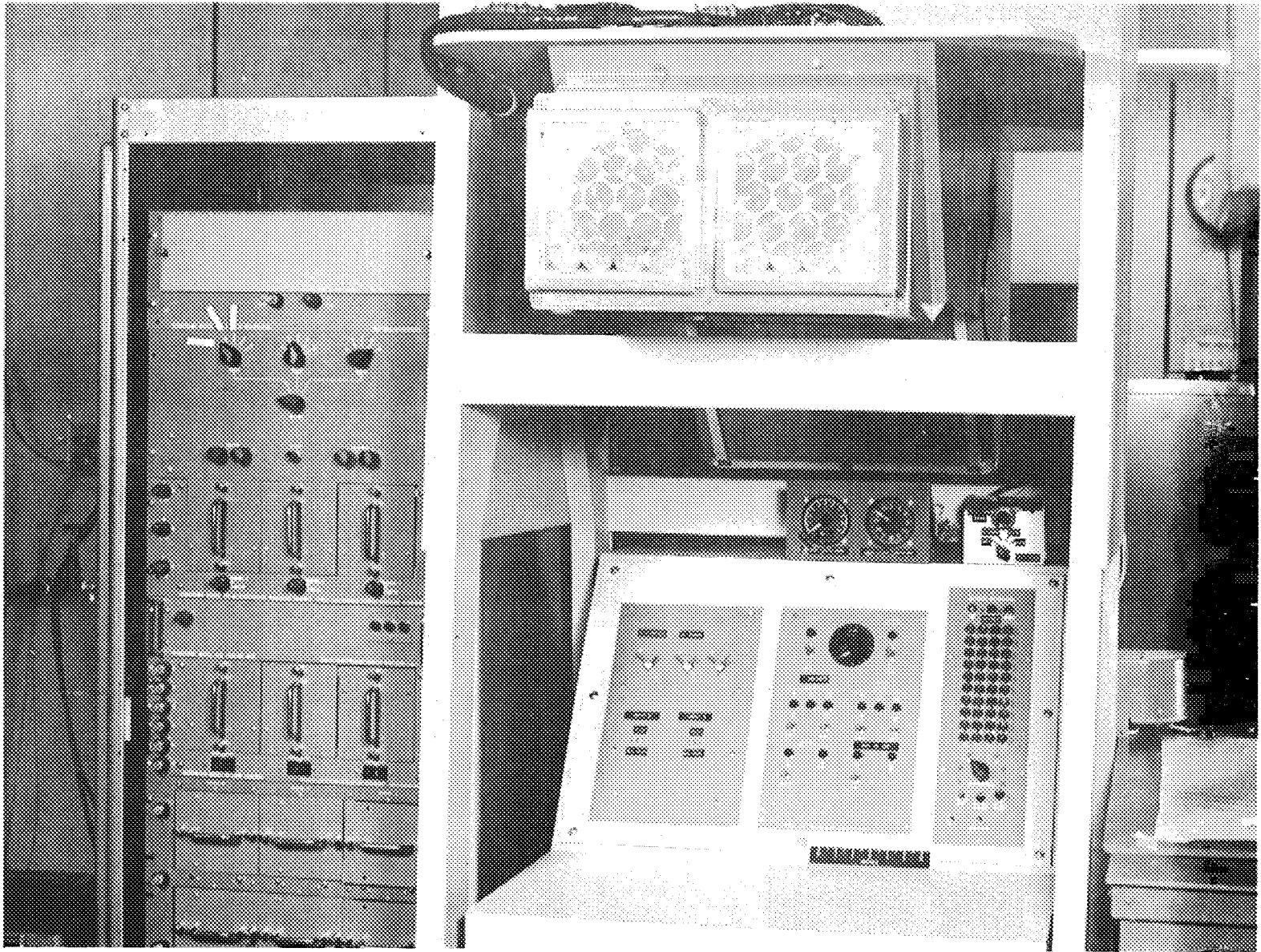


Figure 16.- Preselected runway (10 in. by 15 in. by 15 in. X-Y plotter).

Figure 17. - Final approach altitude versus range (10 in. by 15 in. X-Y plotter).





(a) Complete console.

Figure 18.- Ling-Temco-Vought display system.

(b) 15 in. by 15 in. display screen.
Figure 18. - Concluded.

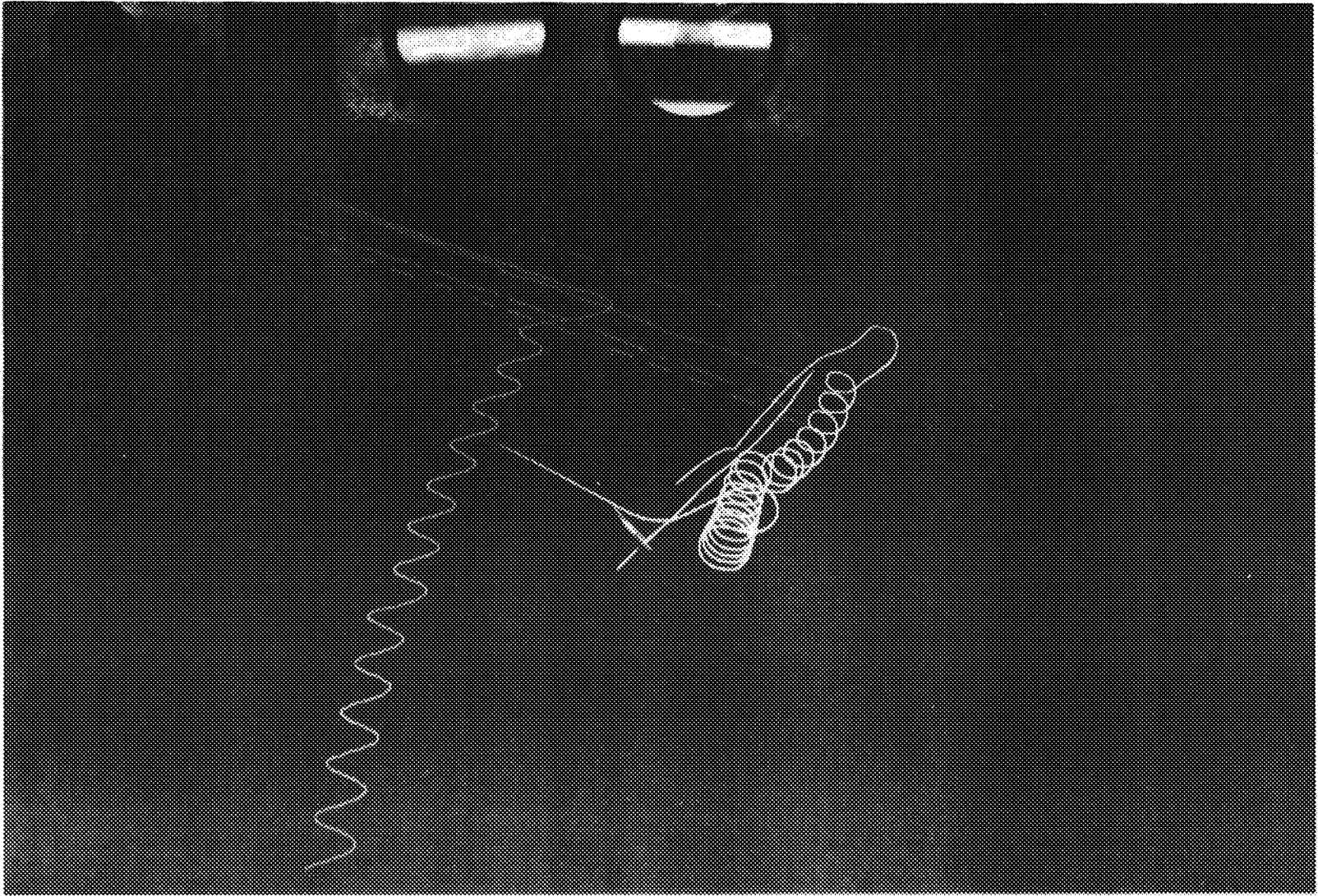
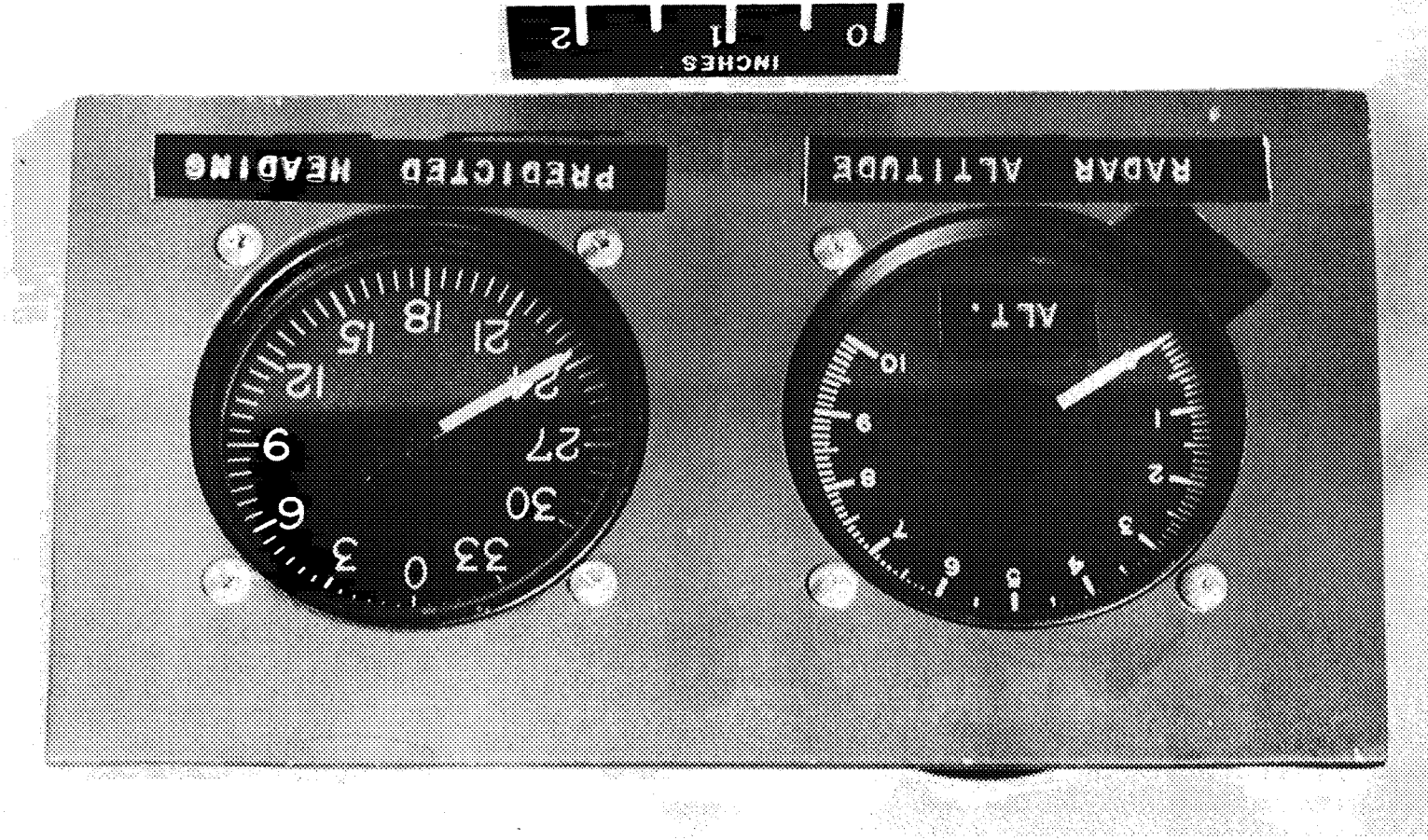


Figure 19. - Radar altitude and predicted heading instruments.



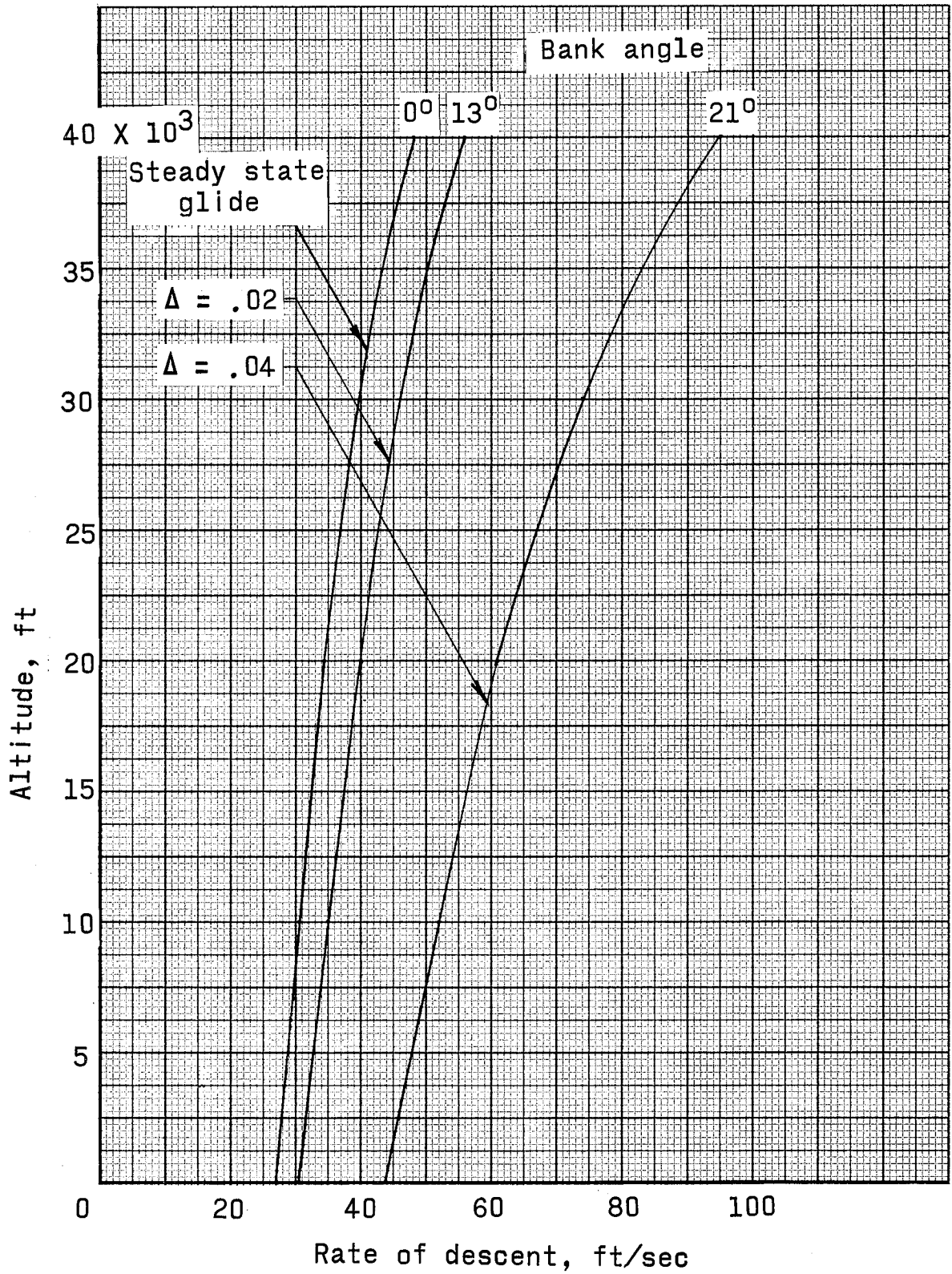


Figure 20.- Altitude versus rate of descent.

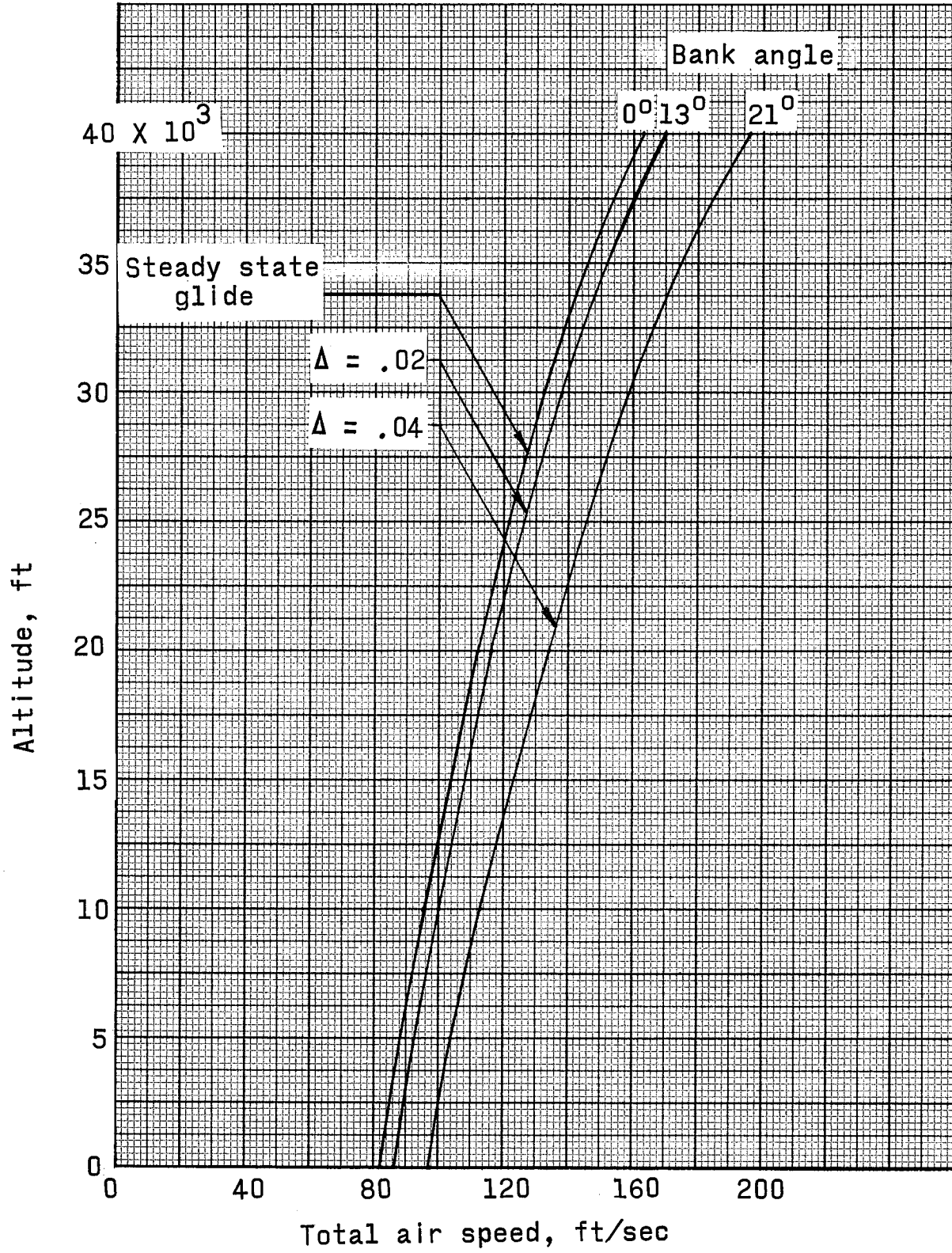


Figure 21.- Altitude versus air speed.

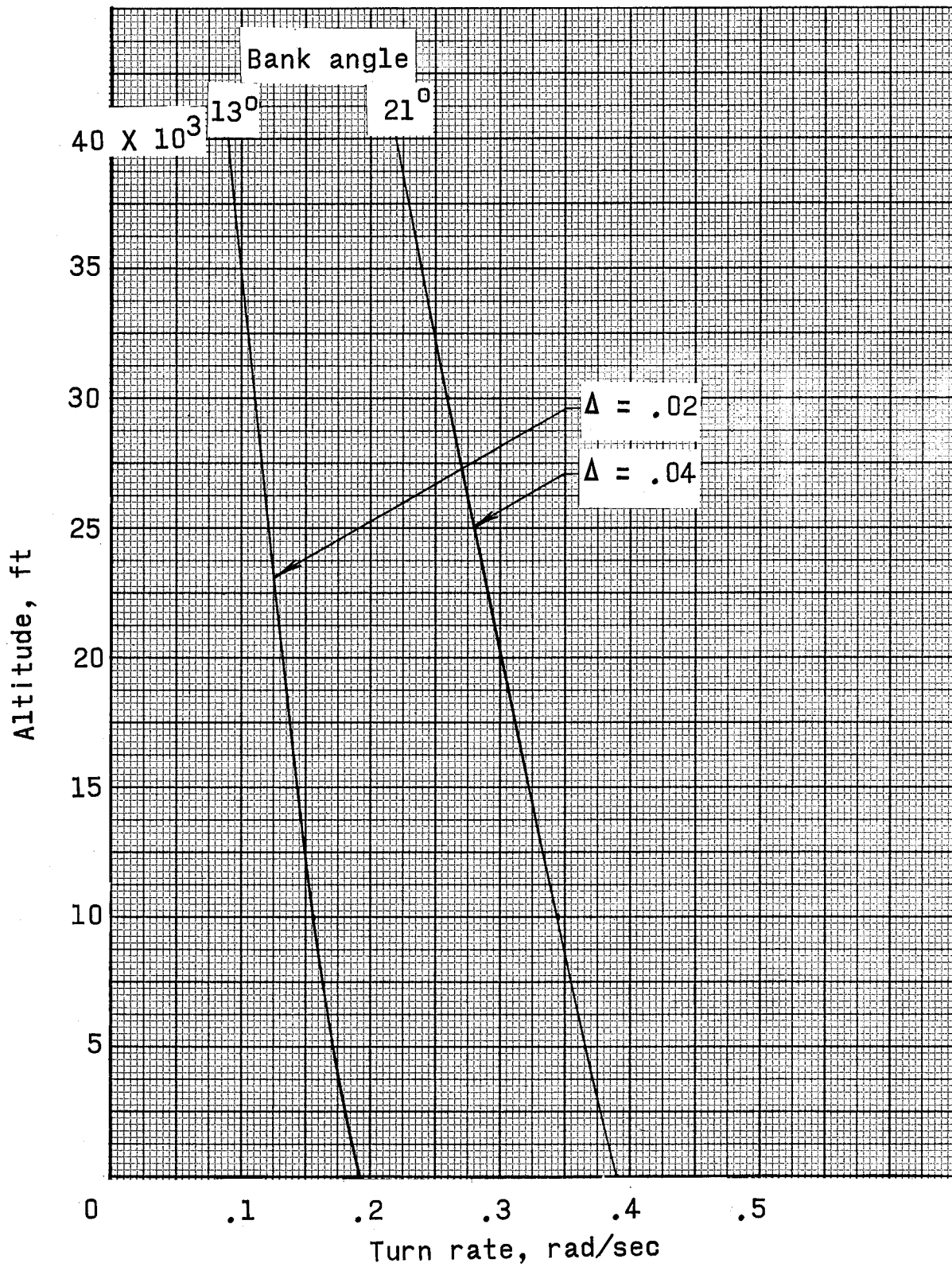


Figure 22.- Altitude versus turn rate.

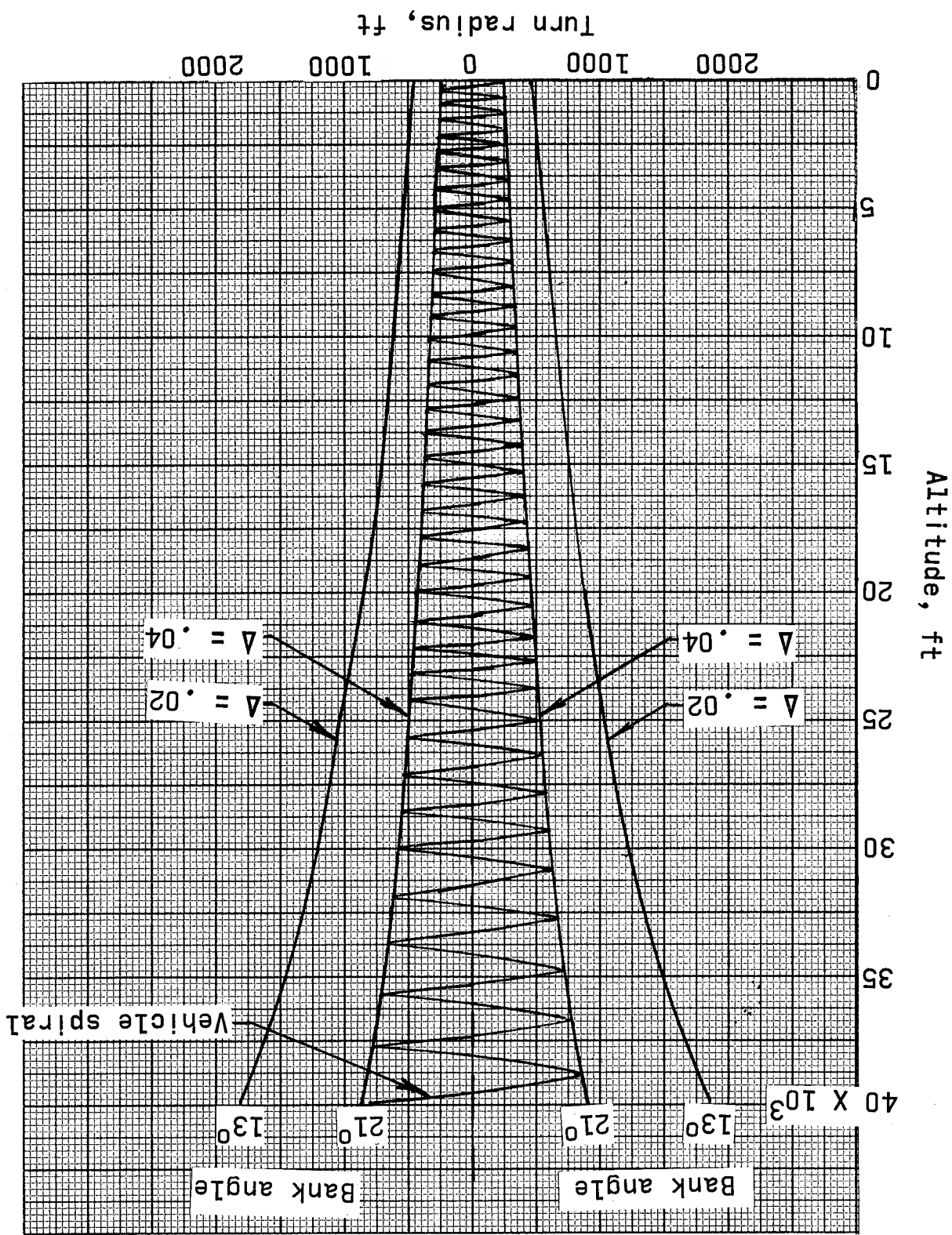


Figure 23.- Altitude versus turn radius.

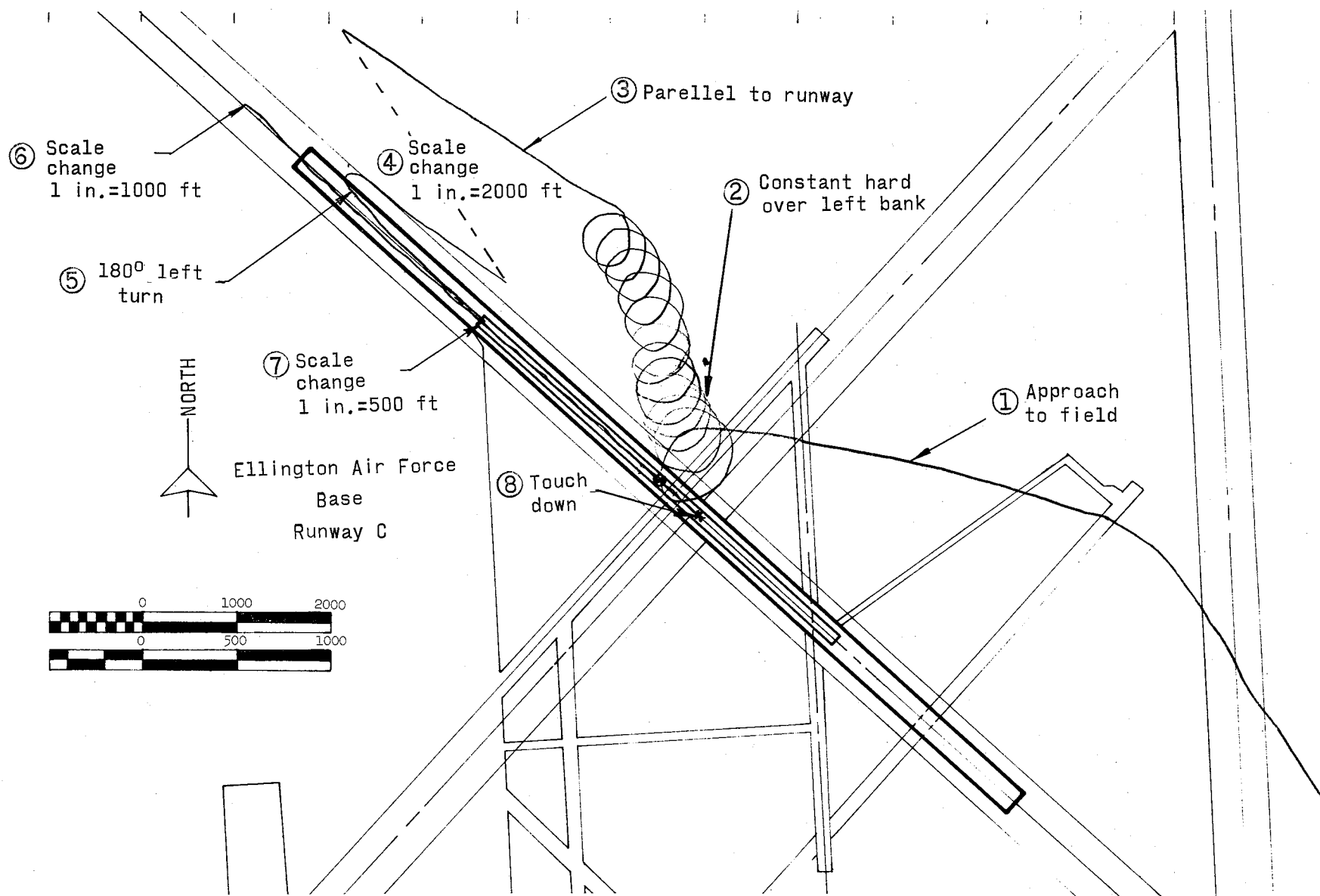


Figure 24.- Ground trace of vehicle (Run A-2).

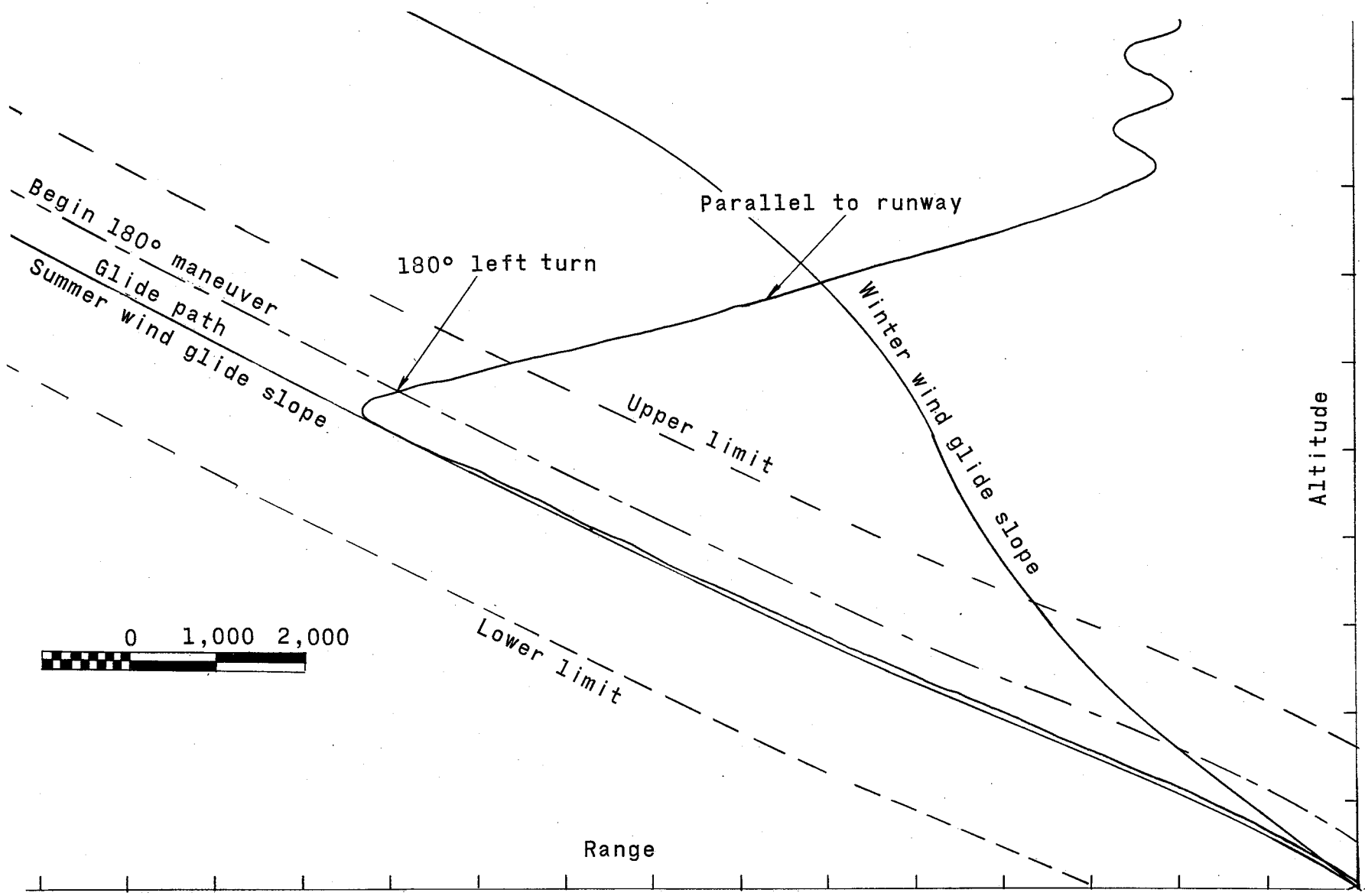
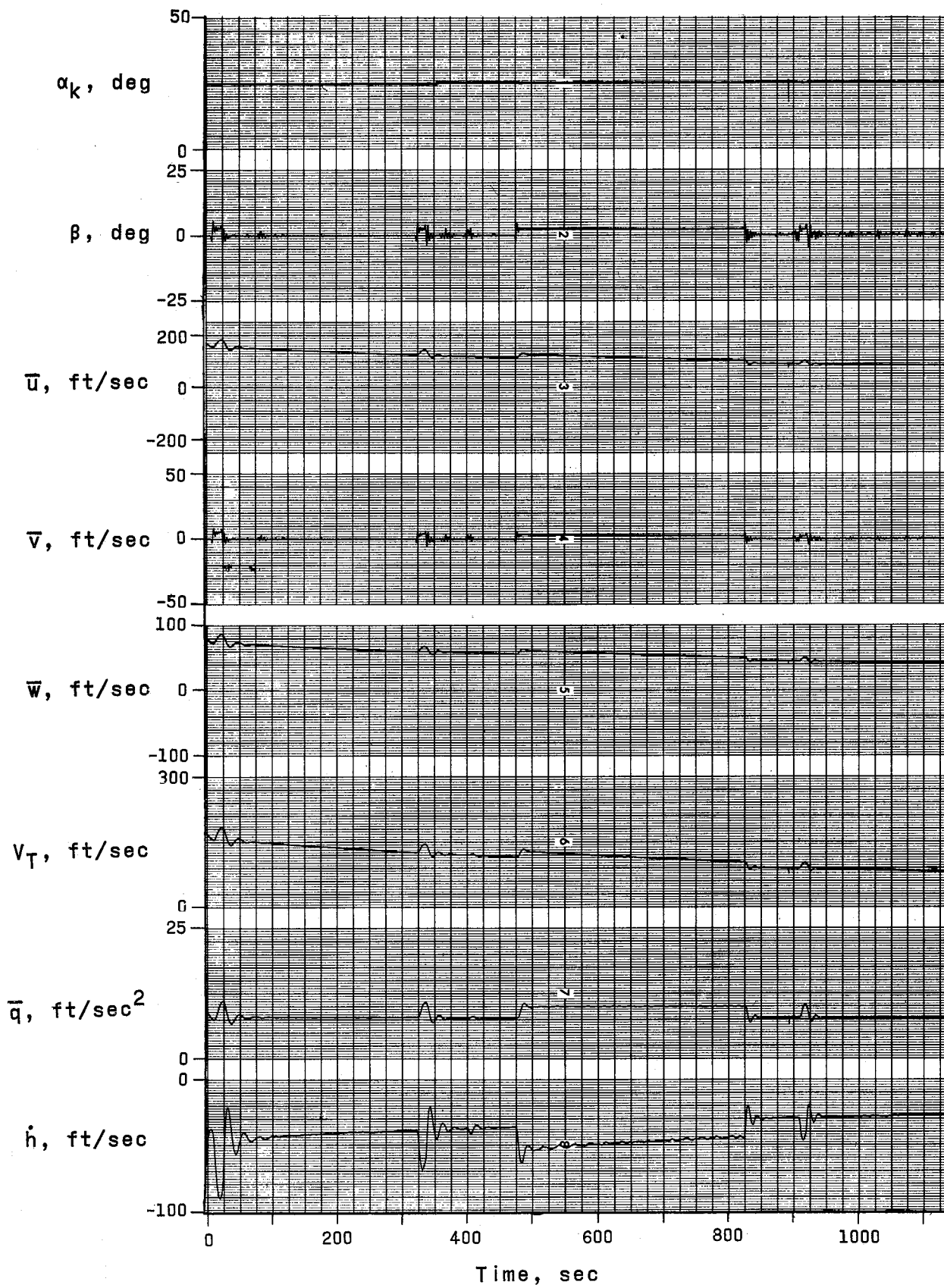
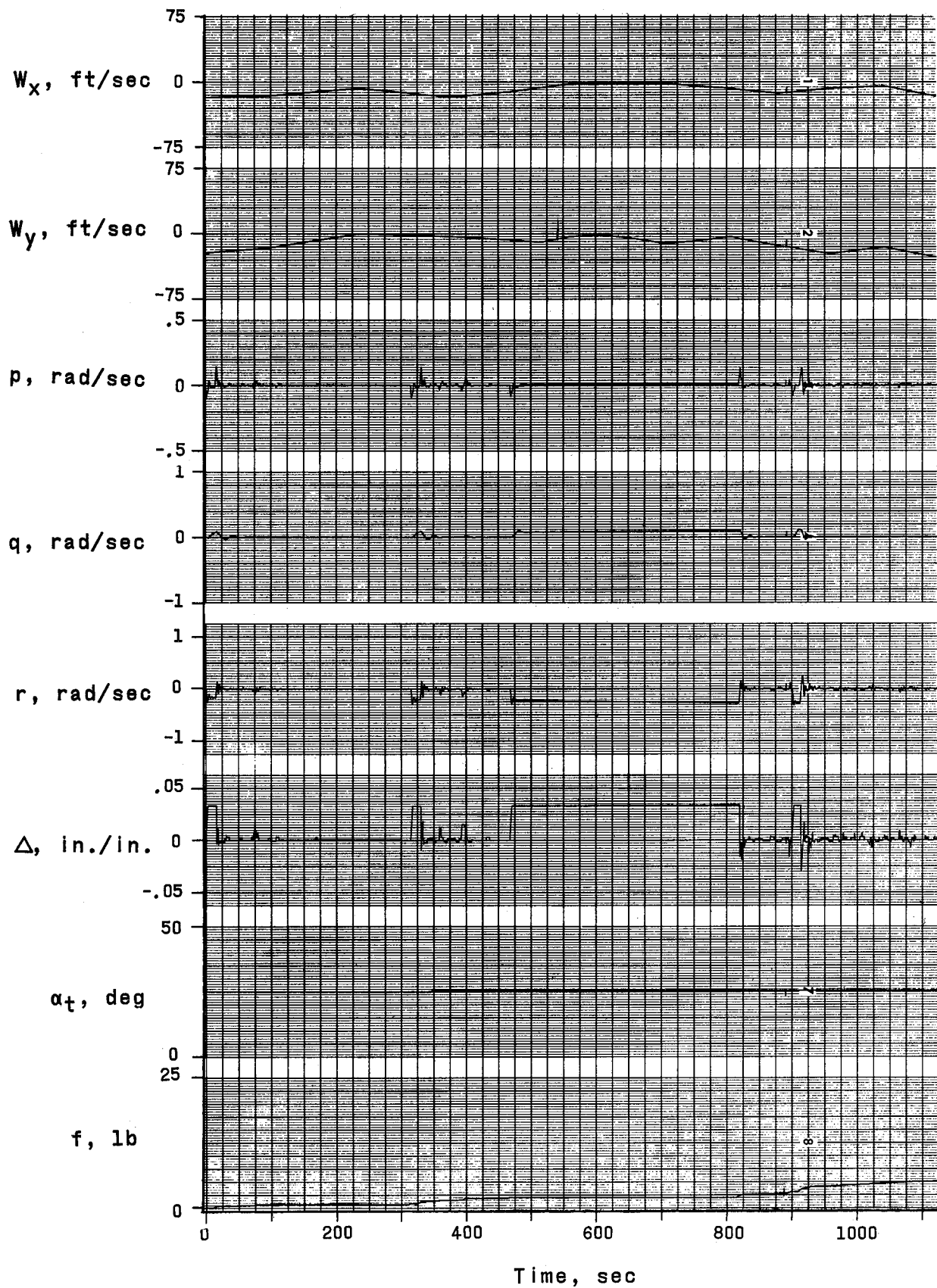


Figure 25.- Altitude versus range trace of vehicle (Run A-2).



(a) Eight channel recorder (A).

Figure 26.- Time histories of terminal descent (Run A-2).



(b) Eight channel recorder (B)

Figure 26.- Concluded.

Altitude at glide slope intersection, ft

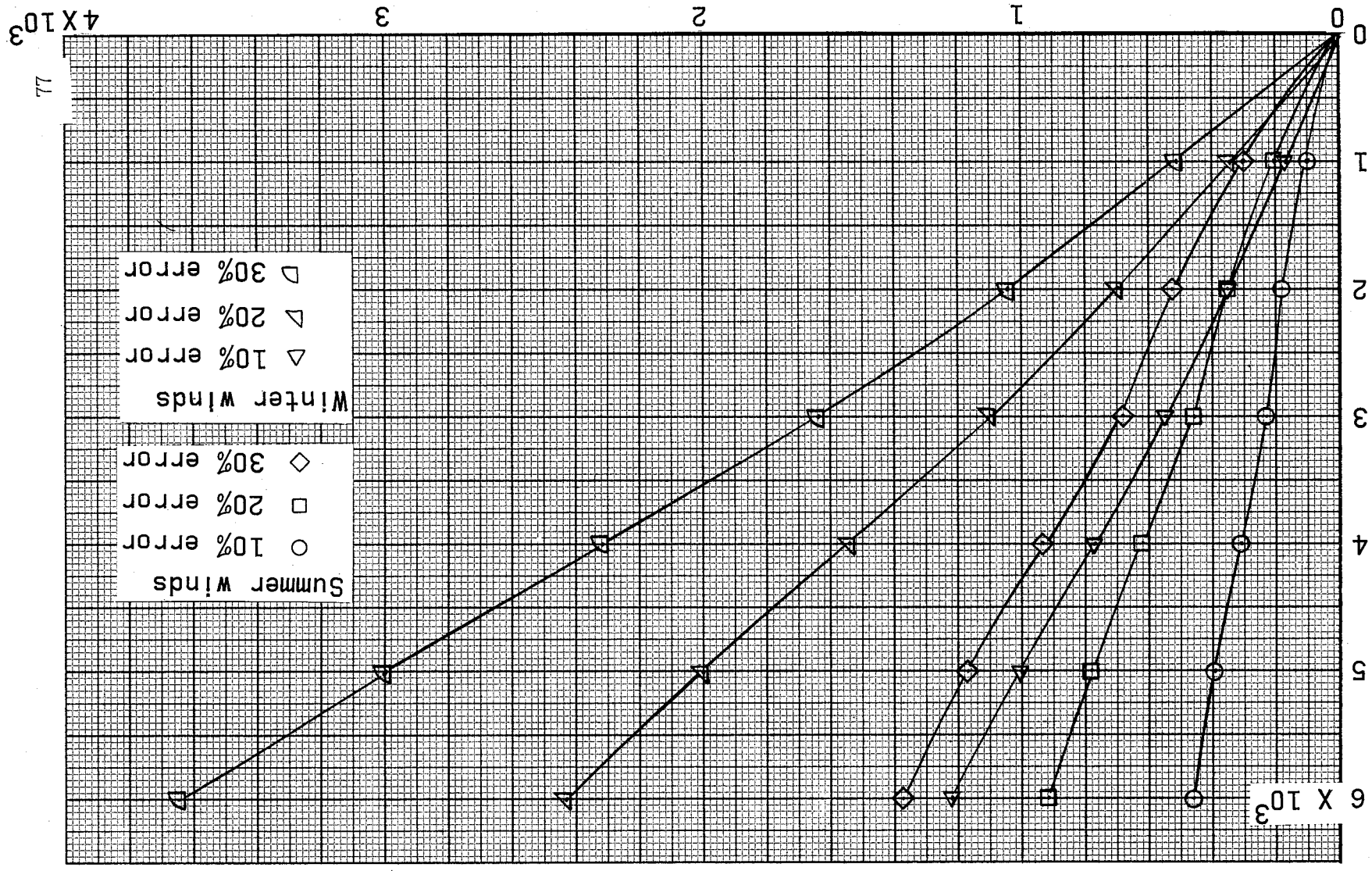


Figure 27. - Miss distance from center of runway, ft during final approach.

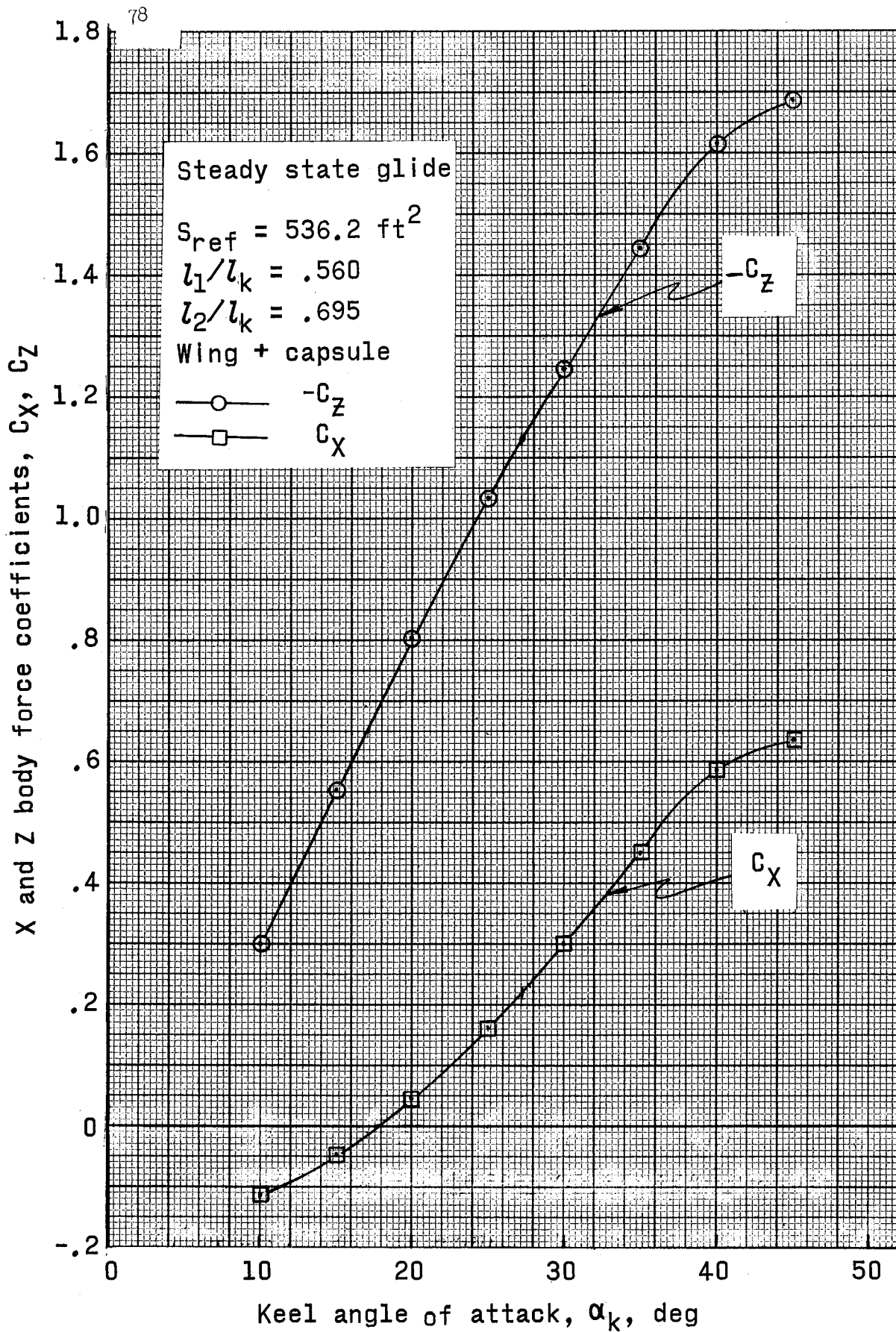


Figure 28.- Aerodynamic force coefficients (C_X , C_Z) versus keel angle of attack (α_k).